HHS Public Access

Author manuscript

Neuroimage. Author manuscript; available in PMC 2019 November 15.

Published in final edited form as:

Neuroimage. 2018 November 15; 182: 136–148. doi:10.1016/j.neuroimage.2017.12.087.

Inferring Brain Tissue Composition and Microstructure via MR Relaxometry

Mark D. Does[a,b,c,d,*]

[a]Department of Biomedical Engineering, Vanderbilt University, Nashville, TN, US

[b]Institute of Imaging Science, Vanderbilt University Medical Center, Nashville, TN, US

[c]Department of Radiology and Radiological Sciences, Vanderbilt University Medical Center, Nashville, TN, US

[d]Department of Electrical Engineering, Vanderbilt University, Nashville, TN, US

Abstract

MRI relaxometry is sensitive to a variety of tissue characteristics in a complex manner, which makes it both attractive and challenging for characterizing tissue. This article reviews the most common water proton relaxometry measures, T_1, T_2, and T_2^*, and reports on their development and current potential to probe the composition and microstructure of brain tissue. The development of these relaxometry measures is challenged by the need for suitably accurate tissue models, as well as robust acquisition and analysis methodologies. MRI relaxometry has been established as a tool for characterizing neural tissue, particular with respect to myelination, and the potential for further development exists.

Keywords

Relaxometry; myelin; microstructure; MRI

1. Introduction

Amongst the many quantitative measurements possible with magnetic resonance imaging (MRI), measurement of water proton relaxation time/rate constants (i.e., *relaxometry*) is amongst the most alluring and beguiling. Relaxation rates in tissue depend on the local physical/chemical milieu in a complex manner, reflecting the molecular constituents of the micro-environment as well as the rates at which water molecules move between different micro-environments. Hence, relaxometry is sensitive to both the sample composition and its microstructure, which makes it attractive for quantitatively characterizing tissue. For example, the relaxation rates in brain are sensitive to the presence of myelin as well as the

*Corresponding author. mark.does@vanderbilt.edu (Mark D. Does).

size of axons. However, the use of practical MRI relaxometry to infer *specific* brain tissue characteristics is hampered by incomplete modeling of the relationships between observed relaxation and tissue composition/microstructure, as well as by the difficulties in accurately and precisely measuring relaxation phenomena. Despite these challenges, the allure persists, and the use of relaxometry to infer brain tissue composition and microstructure remains an active area of research.

This article reviews the development and current state of the most common types of water proton relaxometry, measures of T_1, T_2, and T_2^*. Relaxation effects in the brain due to paramagnetic substances (brain iron, de-oxyhemoglobin, exogenous contrast agents) are not covered, nor are less common relaxometry measures, such as $T_{1\rho}$. Magnetization transfer (MT) is discussed only insofar as necessary to discuss acquisition methods and interpretation of T_1 and T_2 relaxometry. Nonetheless, the scope remains quite broad, and so this article should not be considered a comprehensive literature review. Rather, this is a topic review that aims to distill the salient aspects of MRI relaxometry, specifically for the purpose of inferring the microstructure and composition of myelinated tissue.

The article is organized into three sections, one for each of the types of relaxometry covered. The first and largest section covers T_2 relaxometry of neural tissues, including sub-sections on compartmental modeling, data analysis, and acquisition methods. The subsequent two sections discuss variations of each of these topics in the context of T_2^* and T_1 relaxometry, respectively. Finally, concluding remarks and perspectives are offered on each type of relaxometry and the various manners in which they are implemented.

2. T_2

2.1. The Compartmental Model

T_2 relaxometry was first used to investigate water compartments in excised frog nerve by Swift et al. in 1969 (Swift and Fritz, 1969), and a few years later, Go and Edzes used T_1 and T_2 relaxometry to study edema in brain tissue (Go and Edzes, 1975). The real foundation though for compartment-modeled relaxometry of neural tissue came from Vasilescu and colleagues in 1978 when they analyzed the Carr-Purcell-Meiboom-Gill (CPMG) (Carr and Purcell, 1954; Meiboom and Gill, 1958) signal from excised frog nerve as the sum of three exponential functions (Vasilescu et al., 1978). Based on the time constants (T_2 values) of each function, their signal origins were ascribed to three micro-anatomically distinct water compartments; the assignments, in order of increasing T_2, were reasoned to be "… water closely associated with proteins and phospholipids…" (which one may interpret as myelin, although this specific term was not used), axoplasm, and extra-cellular water.

This multi-compartment interpretation of multi-exponential T_2 (MET_2) relaxation from nerve suggested that it was possible to use T_2 relaxometry to probe neural tissue composition at the microscopic level with great specificity. If the rate of water exchange between these different micro-anatomical compartments was relatively slow, then there was a simple one-to-one relationship between the observed exponential decay functions and corresponding water compartments. With the T_2 value of each function serving to identify

its compartmental origin, the corresponding signal amplitude was then a measure of the anatomical size of the compartment (in terms of water volume fraction). Thus, T_2 relaxometry offered the possibility to independently probe at least three distinct micro-environments of neural tissue, and, for example, measure the volume fraction of myelin.

Of course, the matter was far from settled and numerous challenges remained for the development of neural tissue relaxometry. For one, Vasilescu et al. had also observed temperature-dependent changes in transverse relaxation that were consistent with variations in the rate of magnetization exchange between the compartments, so the slow-exchange assumption was not clear. Also, around the same time, Brownstein and Tarr had demonstrated analytically that multi-exponential relaxation could be derived from a single anatomical compartment with boundary relaxation sinks (Brownstein and Tarr, 1979), which cast doubt on the multi-compartment model.

Following the paper by Vasilescu et al., a number of experimental studies investigated the nature of water proton relaxation in myelinated tissues. Jolesz and colleagues measured T_1 and T_2 in excised degenerating rat sciatic nerve (Jolesz et al., 1984) and in excised myelinated and nonmyelinated nerves of the garfish (Jolesz et al., 1987). They found that the presence of myelin resulted in faster overall relaxation, but these studies did not involve multi-exponential analysis, so while they demonstrated the influence of myelin, they did not directly address the nature of the tissue model. Cadaver samples of human brain were later shown to exhibit MET_2, demonstrating a greater amplitude short-T_2 in white compared to gray matter (Fischer et al., 1990), consistent with the compartmental model. Then, Menon et al. used advances in analysis methods which represented T_2 as a spectrum of amplitudes across a range of T_2 values (Kroeker and Henkelman, 1986; Menon and Allen, 1991; Whittall and MacKay, 1989; Whittall, 1991) (see section 2.2). With this, they performed detailed T_1 and T_2 relaxometry studies on a variety of model neurological tissues (Menon and Allen, 1991; Menon et al., 1992). Through comparison to microscopy, the three largest T_2 spectral components from crayfish nerve cord (see Fig 1) were ascribed to water from axons (component iii in the figure), extra-cellular plus glial space (component ii), and myelin water (component iv). Shortly after, Alex MacKay and colleagues reported MET_2 from human white matter in vivo, and demonstrated it as a method to image myelin water (MacKay et al., 1994). This paper also coined the term, ‘myelin water fraction’ (MWF) to be the fraction of signal decaying with the fast T_2 that is associated with myelin water.

Further support for and insight into the compartmental model of MET_2 came over the years from several studies of different excised animal tissues. Beaulieu et al, revisiting the garfish nerve studies of Jolesz et al., found that the short-T_2 signal component was present only for the myelinated nerves (Beaulieu et al., 1998). Stewart et al. found a reduction in amplitude of the short-T_2 signal in excised samples of brain and spinal cord from guinea pigs with experimental allergic encephalomyelitis—an animal model of multiple sclerosis (Stewart et al., 1993). Does and Snyder found similar results from studies of frog sciatic nerve following the onset of crush-induced Wallerian degeneration (Does and Snyder, 1996). Data from this study (Fig 2) demonstrate the importance of myelin to MET_2, not just as the source of the short-lived T_2 signal, but also as an essential barrier that effectively comparts the tissue into

all the space inside myelinated axons (‘intra-axonal’) and all the space outside myelinated axons (‘extra-axonal’).

An interesting development of the static compartmental model (i.e., ignoring inter-compartmental water exchange) of MET_2 in nerve then came from a combined diffusion-T_2 study of excised frog nerve by Peled et al. (1999). They showed that on a 100 ms time scale, diffusion perpendicular to the axons was restricted for the long-lived T_2 component and unrestricted for intermediate T_2 component. Hence, they argued that the assignment of the two longer-lived components should be reversed—the axonal water resulting in the longer T_2 and the extra-axonal water producing the intermediate T_2 component—and postulated that collagen was responsible for the faster relaxation in the extra-axonal compartment. This conclusion was later supported by the observation that the intermediate T_2 component of excised frog nerve was the first to be affected by the infusion of exogenous contrast agent in the surrounding medium (Wachowicz and Snyder, 2002).

Thus, the basic three pool model of T_2 relaxation of nerve has been well established, although its relationship to white matter relaxation is less clear. In contrast to peripheral nerve, T_2 relaxometry from spinal and cerebral white matter typically resolves into only two signal components (Bjarnason et al., 2005; Dula et al., 2010; Harrison et al., 1995; Kozlowski et al., 2008; MacKay et al., 1994; McCreary et al., 2009; Stanisz et al., 1999; Stewart et al., 1993; Whittall et al., 1997). The explanation for this difference is not known for certain, but one might speculate that because white matter has mostly smaller diameter and more densely packed axons, both the intra- and extra-axonal water will have more frequent interactions and possibly direct exchange of water with the myelin. Whether these interactions are just at the boundary or involve actual exchange of water with the myelin is also not known, but either way the net result is faster and more similarly relaxing water compartments.

Although only two T_2 components are typically resolved in white matter, there is experimental evidence that points to a difference in T_2 between the intra- and extra-axonal compartments. Lancaster et al. used a three pool model with different T_1 and T_2 values to describe white matter intensity in three images with different T_1 and T_2 weightings (Lancaster et al., 2002). Two different studies of excised rat optic nerve reported better characterization of relaxometry data using three compartments with different T_2s (Bonilla and Snyder, 2007; Dortch et al., 2013a). An histology-based computational model was able to explain in vivo T_2 relaxometry from the rat spinal cord using different T_2 values for the intra- and extra-axonal environments, but not if they were constrained to be equal (Harkins et al., 2012). And some recent studies have reported echo time dependence of water diffusion characteristics in white matter (Lin et al., 2017; Qin et al., 2009; Veraart et al., 2017).

Although the intra- and extra-axonal T_2s remain uncertain, it is the short-T_2 component amplitude—the MWF–that has been the primary interest of T_2 relaxometry. In addition to previously mentioned T_2 relaxometry studies of demyelination (Does and Snyder, 1996; Stewart et al., 1993), Stanisz and colleagues undertook a series of MET_2 studies in experimentally injured rat peripheral nerve (Odrobina et al., 2005; Pun et al., 2005; Stanisz

et al., 2001, 2004; Webb et al., 2003). These studies provided extensive data relating variations in nerve microstructure to its MET_2 characteristics, including quantitative correlations of the MWF fraction with histological measures of myelin content (Odrobina et al., 2005; Webb et al., 2003). (One interesting observation from the animal studies is that T_2-defined myelin water does not discriminate between myelin on healthy axons and myelin debris resulting from an ongoing degeneration processes.) Around the same time, similar correlations were found for human white matter by comparing MWF with luxol-fast-blue staining of human cadaver brain samples (Laule et al., 2006; Moore et al., 2000).

The application of MWF imaging in vivo in human studies has been largely done by MacKay, Laule, and colleagues at University of British Columbia. In particular, they have applied MWF imaging in multiple studies of patients with MS as well as a number of other conditions (Lang et al., 2014; Laule et al., 2004, 2007b,c, 2008, 2010, 2016; Kolind et al., 2008; Moore and Laule, 2012; Sirrs et al., 2007; Vavasour et al., 2009, 2017). (A worthy accounting of the work by this group would require a full review article in and of itself.)

Beyond the Slow Exchange Model—The aforementioned MET_2 analyses were based on the slow exchange multi-compartment model. This approach is appealing in its simplicity, but may not hold in all cases, so it is worth considering how T_2 relaxometry is affected by inter-compartmental exchange. An analytical description of relaxation in a system with multiple exchanging compartments is provided in the Appendix, and a more qualitative description is provided here.

The mathematics of the slow exchange model is intuitive: the observed signal is the sum of signals from individual compartments, resulting in multi-exponential relaxation. Consider, for example, two well-mixed compartments of magnetization, with equilibrium amplitudes, M_{0a} and M_{0b}, and relaxation time constants, T_{2a} and T_{2b}. If there is no (or very slow) exchange of magnetization between these compartments, then let the black line in upper left frame of Fig 3 be the T_2 spectrum of this system. The mean T_2s and relative amplitudes of the two components in the spectrum match those of the model. If there is exchange but it is sufficiently slow such that the spectrum does not change appreciably, we say that the system is in the slow-exchange limit. The other extreme, the fast-exchange limit, is also intuitive: magnetization is exchanged between compartments fast enough that the system looks like one well-mixed compartment with mono-exponential relaxation. The green line upper left frame of Fig 3 shows the T_2 spectrum of this example system in the fast exchange limit. Here, the observed relaxation rate, R_{2obs}, is

$$R_{2obs} = \frac{M_{0a}R_{2a} + M_{0b}R_{2b}}{M_{0a} + M_{0b}}, \quad (1)$$

where $R_{2x} = 1/T_{2x}$ for all x.

In between these two extremes, the relationship between the observed signal decay and the compartmental characteristics is more complicated. As exchange increases from the slow to the fast limit, both components in the 2-compartment spectrum shift to the left (lower T_2s),

with the longer-lived component increasing in amplitude and the shorter-lived component decreasing in amplitude. This effect is exemplified in by the blue and orange spectra the upper left frame of Fig 3, where τ_a is the time constant for magnetization remaining in pool 'a'. For systems with more than two compartments (see a 3-compartment example the upper right frame of Fig 3), the scenario becomes even more complex, but left-shift in the T_2 spectrum with increasing exchange remains true.

Looking at the same 2- and 3-compartment example spectra fitted from data with small amounts of noise added (lower frames of Fig 3; SNR = 1000 in these examples), we see how noise may further complicate the interpretation of T_2 spectra. (For more information on fitting of spectra from noisy data, see section 2.2, below.) In particular, while noise simply broadens the components in the 2-compartment example, noise may cause two of the components to blur into one apparent component in the fitted spectrum. The details of these effects obviously depend on the model parameters, but in general, the combination of image noise and inter-compartmental water exchange may make it difficult to interpret a given T_2 spectrum. In the 3-compartment examples in Fig 3, the blurring occurs between the two long-lived components, but under different model conditions, blurring of the two short-lived components can also occur.

With this picture in mind, we can revisit the assumption of the slow-exchange limit for T_2 relaxometry of neural tissue. Many of the early MET_2 studies were aimed at testing the validity of the compartmental model and, in particular, the role of myelin; they were not specifically aimed at quantitatively testing the validity of the slow exchange assumption. Also, many of theses studies were performed on excised nerve (which, as discussed below, likely has slower inter-compartmental exchange than white matter) and at room temperature (also slowing the exchange). Thus, it is not surprising that slow exchange was the starting assumption for MET_2 studies in neural tissue.

In the first detailed report of in vivo MET_2 analysis from human brain, Whittall et al. concluded that exchange had little effect on the T_2 spectrum, because the observed MWF values were in agreement with literature (Whittall et al., 1997). Specifically, they found an average MWF across five white matter regions of 11.3%, which was in close agreement with a previous gravimetric estimate of water mass fraction from human white matter of 10% (Norton and Cammer, 1984). Interestingly though, they also observed significant variations in the T_2 spectra across white matter regions (see Fig 4). In particular, the MWF varied widely (8.4% – 15.0%), and where it was larger, the other spectral component was broader and had a longer mean T_2. Also, as measured by integrating the T_2 spectra, water density did not vary significantly across regions, as one might expect if myelin volume fraction was varying. Looking back at these data now, it is reasonable to postulate that the variations of T_2 spectra across white matter regions were due, at least in part, to variations in inter-compartmental exchange. In fact, this very postulate was put forward a few years hence.

In a study of quantitative magnetization transfer (qMT) in normal human brain, Sled and Pike measured of macromolecular pool size (another putative measure of myelin content) and found that it varied much less across white matter regions than did MWF (as previously reported by Whittall et al.) (Sled et al., 2004). To explain this discrepancy between these two

apparent measures of myelin content, they proposed that the MWF was influenced by inter-compartmental water exchange, which itself might be expected to vary with axon size. To support this postulate, Sled and Pike pointed to a previous combined qMT-MET_2 study that generated a four-pool model of magnetization in bovine optic nerve (Stanisz et al., 1999). Specifically, this model predicted that exchange between the liquid pools (myelin and non-myelin water) at room temperature was sufficient to reduce MWF by 25% from its slow-exchange value. Perhaps because this evaluation was not the focus of the study, the potential importance of this observation was not highlighted by the authors.

Subsequent evidence to support an intermediate-exchange model of MET_2 in white matter has come from a few studies. A simulation study of a four-pool model of white matter magnetization demonstrated that with reasonable model parameters, changes in the rate of inter-compartmental water exchange could substantially alter MWF without having much impact on the qMT-measured macromolecular pool size (Levesque and Pike, 2009). Two experimental studies of rat spinal cord tested the influence of axon size on the T_2 spectrum. Across different white matter tracts of excised and fixed rat spinal cord samples, much like the previous comparisons across white matter regions of human brain, the T_2 spectra, including MWF, were found to vary much more than qMT measures of macromolecular pool size (Dula et al., 2010). Further, histological analysis of the samples demonstrated that these MET_2 variations between white matter tracts were consistent with variations in water exchange rate, as expected due to variations in axon diameter and myelin thickness. The spinal cord MET_2 measurements were later repeated in vivo, with similar observations, demonstrating that the effect was not specific to the ex vivo tissue preparation (Harkins et al., 2012). This same paper also reported histology-based computational modeling which demonstrated that the observed variations in the T_2 spectra across tracts could be explained by variations in myelin thickness given reasonable values of membrane permeability in myelin. To provide a more direct assessment of exchange, methods of relaxation-exchange spectroscopy (Dortch et al., 2009a) were applied in studies of rat optic nerve and frog sciatic nerve (Dortch et al., 2013a). These measurements demonstrated the expected slow-exchange in frog sciatic nerve, but much faster exchange in the rat optic nerve, with rate constants similar to those previously reported in the aforementioned study by Stanisz et al. (Stanisz et al., 1999). Most recently, combined inversion-recovery–CPMG measurements and four-pool modeling of magnetization in bovine white matter has provided similar exchange rate estimates and, consequently, further support for the need to consider the effect of inter-compartmental exchange rates on MET_2 analysis of most types of white matter (Barta et al., 2015).

This is not to say that a clear model for MET_2 relaxation in myelinated tissues exists. In the frog sciatic nerve, which has been well studied, it is probably safe to assume a slow-exchange model. In many other myelinated tissues, including rat spinal cord, rat and bovine optic nerve, and human cerebral white matter, some significant exchange effect likely exists, but studies are ongoing. Most recently, West et al. was able to demonstrate that MWF imaging of fixed rodent brain at 15.2 T can provide reasonably accurate measures of myelin volume fraction, although some signs of inter-compartmental water exchange were evident (West et al., 2016). It is also interesting to note that with the exception of one study in guinea pig brain (Gareau et al., 1999), there are no published accounts of in vivo MWF

imaging in rodent brain. This may be due to the myelin water component simply being lost to exchange at 37 °C in small rodents with relatively thinly myelinated axons in the brain.

2.2. Challenges of Multi-Exponential T_2 Analysis

While modeling continues to be a challenge, perhaps the most fundamental barrier to relaxometry is the ill-posed nature of inverting a sum of exponential functions. Anyone attempting to interpret T_2 relaxometry data should first establish a good understanding of the analysis methods and their inherent limitations. Consider the analysis of a multiple spin-echo measurement with perfect refocusing. Given the multi-compartment, slow-exchange model, the observed spin echo amplitudes, $s(t_i)$, are modeled as equal to the sum of signals from J different compartments plus noise,

$$s(t_i) = \sum_{j=1}^{J} \upsilon_j \exp(-t_i/T_{2,j}) + \eta_i, \quad i = 1 \text{ to } N. \qquad (2)$$

Here, t_i is the i^{th} echo time, υ_j is proportional to the volume of water in the j^{th} compartment, and η is noise. The objective then is to estimate values of υ_j and $T_{2,j}$, $j = 1$ to J, given $s(t_i)$, $i = 1$ to N.

If $J = 1$, the mono-exponential case, there are minor issues related to fitting methods and potential correcting for rician noise, but otherwise the analysis is straightforward and robust. However, as discussed above, transverse relaxation in the brain is not, in general, a mono-exponential process (Whittall et al., 1997). An optimistic perspective might be that mono-exponential T_2 analysis in the brain is a good example of effective biased estimation (Kay and Eldar, 2008), where precision of the estimated parameters are improved at the cost of inaccuracy. For example, a fast and precise mono-exponential T_2 mapping of the brain might prove to be a valuable tool to screen for abnormal tissues or subtle changes over time. Also, a mono-exponential model opens the door to faster acquisition methods, including steady-state methods (Deoni et al., 2003; Schmitt et al., 2004) and various model based reconstructions (Ben-Eliezer et al., 2015; Huang et al., 2013; Lankford et al., 2015; Ma et al., 2013; Sumpf et al., 2011, 2014). For quantitative characterization of white matter microstructure and composition though, a scalar T_2 estimate cannot capture much of a slowly-exchanging multi-compartment model. Also, since the resulting bias will depend on the acquisition protocol, there is the problem that one protocol may provide a different estimate of T_2 than another, making multi-site comparisons difficult.

Consequently, to characterize brain tissue with T_2 relaxometry, the multi-exponential case, $J > 1$, is likely required. In this case, the analysis becomes significantly more difficult, both in terms of inherent precision and, if non-linear regression methods are used, ease of convergence. This problem has been extensively studied outside the application of MRI relaxometry (Bertero et al., 1985; Istratov and Vyvenko, 1999) and has been evaluated by numerical simulations specifically for the purpose of characterizing white matter by T_2 relaxometry (Bjarnason et al., 2009; Fenrich et al., 2001; Graham et al., 1996). The most common approach used for NMR/MRI relaxometry is to formulate the problem into a linear

system and fit a spectrum of amplitudes (e.g., a T_2-spectrum) corresponding to exponential functions spanning a T_2 domain which is broad and dense enough to account for all expected signals (Whittall and MacKay, 1989). That is, re-write Eq (2) as **s** = **Av**, where **s** is a column vector of echo amplitudes, **v** is the T_2-spectrum, and the columns of **A** are decaying exponential functions spanning the expected T_2 domain. In general, this linear system is highly ill-conditioned, so constraints must be applied to solve for **v**.

Many cases of MRI relaxometry, such as T_2 relaxometry from a multiple spin echo measurement, are consistent with the constraint that all the values in **v** are non-negative. Applying this constraint greatly improves the system conditioning, and Lawson and Hanson's non-negative least squares (NNLS) algorithm (Lawson and Hanson, 1995) provides a simple and robust method for computing this constrained inverse. However, even with the non-negativity constraint and perhaps also some type of Tikhonov regularization of the spectrum (Whittall and MacKay, 1989; Whittall et al., 1991; Borgia et al., 1998, 2000), SNR demands are still high. For example, one simulation study of white matter at 1.5 T (a two-compartment system with $v_1 = 0.1$, $T_{2,1} = 15$ ms, and $T_{2,2} = 100$ ms) indicated that with an acquisition of 32 echoes at 8 ms echo spacing, an SNR ≈ 500 is needed to identify the the correct number of components 90% of the time and to estimate the short-T_2 component amplitude with 10% coefficient of variation (Graham et al., 1996). These high SNR demands become greater if the underlying T_2 components have broader widths and/or less relative separation in the T_2 domain (Fenrich et al., 2001). It is possible to lower the practical SNR requirements by trading-off spectral or spatial resolution in various ways (Dortch et al., 2013a; Hwang et al., 2011; Jones et al., 2003b, 2004; Kwon, Oh In et al., 2010; Raj et al., 2014; Stanisz and Henkelman, 1998; Whittall and MacKay, 1989; Vidarsson et al., 2005), but the inherent ill-posed nature of the problem cannot be overcome by better analysis methods. Thus, the starting requirement for all multi-exponential relaxometry is a relatively high image SNR, which in-turn dictates some combination of large image voxels and long acquisition times, neither of which are desirable.

The difficulty in T_2 spectral analysis is further complicated by a number of other fitting and analysis choices, which, naturally, are made more difficult at moderate to low SNR. Choosing the lower boundary of the T_2 domain can be a challenge when the time of the first sample (t_1) is similar or longer than the shortest time constant within the signal, as is typically the case for myelin water imaging. This was looked at through simulations by Fenrich (1992) for a variety of underlying signal and noise characteristics, but there is no definite solution and experience dictates that MWF estimates, for example, can varying depending on the choice of this boundary. Choosing the type and level of spectral regularization may also be a problem. These choices will dictate the shape of the fitted spectrum, and goodness-of-fit measures like the χ^2 statistic cannot identify which shape is most accurate (Whittall et al., 1991; Borgia et al., 1998). For example, multiple adjacent spectral components does not necessarily indicate two distinct signals, but rather could be from one broad distribution of T_2 components. Spectral regularization can be avoided altogether, which was recommended by Bjarnason et al. based on simulations (Bjarnason et al., 2009), but Levesque et al. commented that reduced regularization did not necessarily result in more reproducible results (Levesque et al., 2010). The discrepancy here may reflect

the fact that the underlying T_2 spectrum is better described by smooth components of finite width (thereby necessitating some regularization) rather than the discrete bi-exponential relaxation used in Bjarnason's simulations. Without independent gold-standard knowledge of the underlying T_2 spectrum, there is, again, no definitive and general solution to this problem.

A related challenge lies in choosing a method for extracting metrics of interest from the fitted T_2 spectrum. For example, to extract a MWF estimate, does one simply compute the fraction of signal below a cut-off T_2 value or segment the spectrum at points of local minimum and include only components with mean T_2 below a cut-off, and either way, how is the cut-off value determined? The sensitivity of choosing a MWF cut-off T_2 value is exemplified in the Levesque et al. report on reproducibility of myelin water imaging (Levesque et al., 2010). This report paints a less than rosy picture of clinical use of myelin water imaging, based primarily on these multitude of processing challenges. A more recent multi-site study, done at higher field (3 T) and using newer, more robust acquisition methods (see below), reported better measures of reproducibility (Meyers et al., 2013), but it is safe to say that there is room for more work on optimizing and evaluating the analysis of multi-exponential relaxometry data.

2.3. Acquisition Methods

A recent technical review of myelin water MRI includes the necessary material for T_2 relaxometry with MRI (Alonso-Ortiz et al., 2015), but a somewhat more general and less technical overview is also provided here for completeness.

Most of the early relaxometry studies involved isolated tissue samples, thereby avoiding the need for spatial encoding and providing relatively high SNR. Also, these measurements used high-bandwidth 'hard' RF pulses capable of generating relatively accurate RF refocusing of magnetization across the entire sample, and remaining inaccuracies were often largely resolved through RF phase-cycling. Thus, in terms of both precision and accuracy, these studies provided a near gold standard for relaxometry. However, for in vivo evaluation or even ex vivo evaluation of a whole brain or large brain sections, relaxometry needed to be extended into the realm of imaging, which presented multiple challenges. The need to spatially-localize the signal introduces longer scan time, lower SNR, and signal model complications associated with slice selective pulses. Efforts to address one of these problems (e.g., scan time) often exacerbates one or more other problems (e.g., model accuracy and SNR). Current methods make use of modern computing power to mitigate these problems, but fast and effective MRI relaxometry remains an area of active research and development.

Multiple Spin Echo MRI—As shown in a series of papers in the 1980s (Crawley and Henkelman, 1987; Majumdar et al., 1986a,b) the CPMG method for measuring T_2 is not immediately translatable to MRI. The problem is that the use of slice-selective RF refocusing pulses and/or spatial variations of B_1^+ and B_0 over the imaging volume dictate some significant degree of imperfect refocusing, which in-turn means that the exponential signal model in Eq (2) is not an accurate representation of the observed signal. The solution adopted at the time was to use non-selective (rectangular or composite) refocusing pulses

and amplitude/direction-modulated spoiler gradients (Barker and Mareci, 1989; Crawley and Henkelman, 1987; Majumdar et al., 1987) to minimize signals from non-CPMG coherence pathways. These approaches were brought together and refined by Poon and Henkelman (1992), which then defined the standard acquisition framework for MRI T_2 relaxometry, particularly when multi-exponential analysis was needed. Shortly after, Alex MacKay and colleagues implemented a variation of this method with 10 ms echo spacing and 32 echoes, and applied the linear inverse multi-exponential analysis to fit T_2-spectra on a voxelwise basis, resulting in the first in vivo human demonstration of myelin water imaging (MacKay et al., 1994).

Although MacKay and colleagues (as well as a few others) made effective use of this MRI T_2 relaxometry protocol (Kolind et al., 2008, 2009; Laule et al., 2004, 2006, 2007b,c, 2008; Mädler et al., 2008; Vavasour et al., 2009; Whittall et al., 1997), it had several shortcomings. Most importantly, scan times were long (25 min, Whittall et al. (1997)) and coverage was limited to a single-slice. Also, while the modulated spoiler gradients could, in principle, remove all the non spin-echo signals, in practice, the gradient amplitudes necessary to de-phase signals across a slice were not attainable on clinical scanners, and a strategy to reduce this requirement was limited and came with an SNR penalty (Does and Snyder, 1998). Further, even if the unwanted signal could be entirely removed, the measured (apparent) T_2 was still a function of the effective refocusing pulse angle. Thus, the imaging slice location was restricted to orientations/offsets that provided relatively uniform B_1^+, otherwise the apparent T_2(s) would vary across the slice. This was less of a problem in the early studies at 1.5 T but became more of a challenge as 3.0 T became the standard (Kolind et al., 2009). As a consequence of these acquisition limitations, as well as the aforementioned analysis/SNR challenges, multi-exponential T_2 relaxometry with MRI was not widely adopted.

A few improvements and alternative approaches were presented. To reduce scan time, the simple approach of reducing TR was found to impart little bias in the resulting MWF maps (Laule et al., 2007a), but of course this had limited benefit and involved an SNR cost. Likewise, acquiring multiple lines of k-space per echo (i.e., gradient and spin-echo acquisition—GRASE) was evaluated (Does and Gore, 2000b), but this too came with an inherent SNR penalty. Higher magnetic fields helped address the SNR challenges, but exacerbated the B_1^+ problems (Kolind et al., 2009), as noted above.

In order to increase coverage, large-slab magnetization preparation was combined with multi-slice low-excitation flip angle read-out (Oh et al., 2006). This approach also included an SNR cost and remained sensitive to B_1^+ variation, but permitted efficiency improvement through non-linear sampling of the echo time domain (Bertero et al., 1985; Shrager et al., 1998) which is not suitable for conventional multiple spin-echo acquisitions (Does and Gore, 2000a). A recent modification of the T_2-prep approach has used adiabatic refocusing pulses to mitigate effects the B_1^+ variation (Nguyen et al., 2016). The result was high quality, whole brain MWF at 3.0 T in 4 min. As noted by the authors, the adiabatic pulses and limited echo-time sampling introduce complications and limitations, but the results are nonetheless impressive. It remains to be seen if this approach will become widely adopted though,

because, as discussed below, it is now known that B_1^+ can simply be incorporated into the signal model.

In general, the observed multiple spin-echo signal is a function of four parameters: equilibrium magnetization (M_0), relaxation time constants T_1 and T_2, and the refocusing pulse flip angle (θ). By removing and/or avoiding signal contributions resulting from $\theta \neq 180°$, previous acquisition methods had reduced the signal to conform to an exponential model, dependent on only M_0 and T_2. However, because i) there is little dependence of the signal on T_1 and ii) θ and T_2 are relatively independent model parameters, it turned out to be possible to constrain T_1 to a reasonable value and then fit M_0, T_2, and θ from a multiple spin echo measurement. These important observations were first reported by Jones et al. in a forgotten/overlooked conference abstract (Jones et al., 2003a) and then independently re-discovered and published by Lebel and Wilman (2010). This paper also demonstrated that the joint fitting of M_0, T_2, and θ was applicable to slice selective acquisitions, given a known refocusing pulse slice profile. Thus, use of a signal model that includes flip angle has effectively removed the barriers associated with B_1^+ variation and slice selection for multiple-spin echo T_2 relaxometry.

Follow-up works have included a number of developments. Most importantly, the θ-dependent signal model was demonstrated to also be effective for MET_2 analysis (Prasloski et al., 2012a). Applications of the analysis has since been used to demonstrate volumetric myelin water imaging through 3D (Prasloski et al., 2012b) and multi-slice (Akhondi-Asl et al., 2015) acquisitions. Both of the original reports of θ-dependent analysis (Jones et al., 2003a; Lebel and Wilman, 2010) used the extended phase graph signal model (Hennig, 1988), but the echo generating function (Lukzen et al., 2009; Sumpf et al., 2011) or simply the Bloch equations can also be used (Akhondi-Asl et al., 2015; Ben-Eliezer et al., 2015). The benefit of using accurate, flip-angle defined slice profiles rather than a Fourier approximation has been evaluated experimentally (McPhee and Wilman, 2017), and using an analytical propagation of error analysis, the idea of independently measuring, rather than jointly fitting, θ has been evaluated theoretically (Lankford and Does, 2017).

2.3.1. Gradient Echo—Gradient echo pulse sequences offer a number of advantages over the multiple spin echo approach. Gradient echo sequences are readily accelerated by reducing TR and excitation flip angle, which in-turn accommodates 3D encoding and mitigates the RF power deposition challenges of multiple spin echo sequences. Also, with no need for RF refocusing pulses, a larger fraction of scan time can be spent acquiring data, which corresponds to an SNR efficiency advantage. Moreover, without an RF refocusing pulse, signal acquisition can begin sooner after excitation, which is particularly advantageous when trying to characterize the rapidly decaying myelin water signal.

Gradient echo sequences come in two general flavors: incoherent (aka ‘spoiled’) and coherent. The spoiled gradient echo pulse sequence provides T_2^*-weighted images, and, as such, is discussed in the T_2^* section, below. Alternatively, a coherent sequence with balanced gradient waveforms can provide images with contrast that depends on T_1 and T_2, and thus

can be used for T_2 relaxometry given independent knowledge of T_1. This approach, with independent (or jointly fitted (Teixeira et al., 2018)) T_1 estimates derived by variable-flip-angle spoiled gradient echo imaging, has gained widespread traction for single component rapid T_1 and T_2 relaxometry (known as DESPOT1 and DESPOT2) (Deoni et al., 2003).

An extension of this method to a multi-compartment model for characterizing white matter (called mcDESPOT) promised to estimate the T_1s, T_2s, relative sizes, and inter-compartmental exchange rate of a two-compartment system (Deoni et al., 2008). However, a theoretical analysis showed that with unconstrained signal analysis this approach cannot provide parameter estimates with useful levels of precision (Lankford and Does, 2013). The same analysis showed that model constraints, including neglecting inter-compartmental exchange, may improve precision at the cost of parameter inaccuracy, but a particularly useful combination of model parameters and constraints was not found. Similar results were found by Monte Carlo simulation (Bouhrara et al., 2016), and an in vivo experimental study found that MWF from the mcDESPOT approach could not be considered equivalent to those from multiple-spin echo imaging (Zhang et al., 2015a). Lankford and Does had postulated that MT effects, having been previously demonstrated to alter contrast in gradient echo sequences (Bieri and Scheffler, 2006; Crooijmans et al., 2011; Gloor et al., 2008; Lenz et al., 2010; Ou and Gochberg, 2008), might be affecting the mcDESPOT signals in a manner that was not included in the model. Indeed, MT effects in mcDESPOT signals were demonstrated experimentally in human brain, and thus remain an unresolved complication to this approach (Zhang et al., 2015b). Recently, Bouhrara et al. have proposed a Bayesian analysis framework for mcDESPOT (while neglecting inter-compartmental exchange and magnetization transfer) (Bouhrara and Spencer, 2016), which shows promise for effective MWF and relaxation time imaging in human brain (Bouhrara and Spencer, 2017). Time will tell whether this, or other gradient echo based methods, are able to supplant the established multiple-spin echo methods for multi-compartment T_2 relaxometry.

3. T_2^*

An alternative type of relaxometry, which aims to combine the benefits of gradient echo imaging with the relative sensitivity of multi-spin echo T_2 measurements, is multi-exponential T_2^* analysis of multiple (spoiled) gradient echo images. In the simplest form, a multi-exponential T_2^* (MET_2^*) model can be made identical to the MET_2 model presented in Eq (2), with T_2^* replacing T_2. Such an approach was used by Du et al. to demonstrate the potential for MET_2^* to generate MWF maps (Du et al., 2007). However, in most cases, MET_2^* analysis requires corrections for additional signal variations that are not present in spin echo images.

Without RF refocusing, the echo-time dependence of the multiple gradient echo signal is sensitive to magnetic field variations across and within the voxel, from the micro- to the macro-scopic scales (Yablonskiy, 1998). The intention of relaxometry is to characterize the tissue at the sub-voxel level, so the effects from the larger scale field variations are not of interest. A first-order characterization of these field variations assumes they are linear in

space (i.e., are gradients in the X-, Y-, and Z-directions), in which case they impart a sinc function modulation on the observed multiple gradient echo signal. In order to apply accurate MET_2^* analysis, this sinc modulation must be substantially reduced or removed.

Lenz et al. attempted to mitigate the background gradient effect by imaging at 1.5 T, employing careful 2nd-order shimming, and using 3D encoding with near isotropic voxel dimensions (~ 2 mm), but the resulting MWF values were still low compared to those from MET_2 analysis. Others have used estimates of the background field gradients to estimate and correct for their effects. Hwang et al. used a multi-slice 2D acquisition at 3 T, with 4 mm slice thickness and ~ 0.1 mm in-plane resolution (Hwang et al., 2010). With this geometry, the in-plane background field gradients were assumed negligible, and then the through-plane gradients were estimated by finite difference of the field maps of adjacent slices, where the field maps came from the phase shift of images at two echo times. More recently, Alonso-Ortiz et al. fitted the sinc modulation function from later echoes where the underlying signal decay was assumed mono-exponential (Alonso-Ortiz et al., 2017a). The sinc modulation was then divided out of the signal at all echo times, and then a linear inverse MET_2^* was performed. This approach was then found to provide MWF values that were in close agreement with those from multiple spin echo measurements, although with somewhat lower SNR (Alonso-Ortiz et al., 2017c).

Other complicating factors in MET_2^* analysis relate to the compartment-level differences in the gradient-echo compared to the spin-echo signal. For one, compartment-level variations in magnetic susceptibility will alter the gradient echo signal model. Mapping magnetic susceptibility itself is of interest for characterizing brain tissue (for more information, see this recent review (Duyn, 2017)), but for MET_2^* signal analysis, susceptibility-induced frequency shifts (Δf) become orientation-dependent and compartment-specific terms in the multi-compartment signal model. Hence, rather than a linear inverse analysis, the complex gradient echo signal should perhaps be modeled as the sum of signals, each with a unique amplitude, T_2^*, and Δf (Nunes et al., 2017; Sati et al., 2013; van Gelderen et al., 2012). For a 3-compartment model, it has been demonstrated that the inclusion of these frequency terms improves fitting of a multi-gradient echo signal (Nam et al., 2015). However, another study determined that, given sufficient SNR and with the narrower objective of estimating MWF, the effect may be ignored in favor of linear inverse analysis at static fields strengths of 3 T and below (Alonso-Ortiz et al., 2017b).

A second compartment-level signal difference between gradient- and spin-echo signal may offer an advantage for T_2^*- over T_2 relaxometry. In general, T_2^* relaxometry is subject to the same, previously discussed, complications related to the exchange, but to the extent that $T_2^* \leq T_2$ at the compartment level (i.e., not simply due to meso- or macroscopic field variations), its shorter relaxation times make it less sensitive to the effects of inter-compartmental water exchange. This idea was noted in a recent comparison of MET_2^* and MET_2 for myelin water imaging (Alonso-Ortiz et al., 2017c), but remains to be evaluated.

4. T_1

4.1. The Compartmental Model

While the slow-exchange model allows MET_2 and MET_2^* relaxometry to probe the individual compartments of neural tissue, or myelin at least, T_1 relaxometry has been used to characterize neural tissue using both mono- and multi-exponential analyses. Before delving into the various approaches though, consider the necessary model components, which are more complicated than those necessary for transverse relaxation. First, as with T_2 and T_2^*, we expect that water in myelin and non-myelin compartments will have different intrinsic T_1s. Second, in addition to water compartments, it is necessary to consider macromolecular protons, which exchange magnetization (i.e., MT) with the water protons, resulting in bi-exponential relaxation for a given compartment of water and macromolecules (Edzes and Samulski, 1978; Gochberg et al., 1997). Thus, modeling longitudinal relaxation in myelinated tissue, one might want to start with four proton pools (myelin and other water, and their associated macromolecular pools), as first used by Harrison et al. (1995), resulting in relaxation that is best described by a quad-exponential function. Also, as discussed above, the rate of exchange between the water pools may be important, so the four-pool model should include coupling between the two water pools as well as between each water pool and its associated macromolecular pool. This makes for a rather complicated model which is unlikely to be invertible with data from a clinically compatible MRI protocol; consequently, a simplified model is necessary and a few different approaches have been used.

One approach to simplify the model is to reduce all the water protons into one pool and all macromolecular protons into another. Although the macromolecular protons signals are not directly observed, because of MT, the water proton longitudinal relaxation in this model will be bi-exponential (Edzes and Samulski, 1978; Gochberg et al., 1997). This approach has been developed and applied for MRI (Dortch et al., 2011, 2013b; Gochberg et al., 1999; Gochberg and Gore, 2003, 2007), but is not discussed in detail here, as MT imaging of brain is the subject of another review (Sled, 2017).

A second approach to simplifying the model of longitudinal relaxation is to ignore the MT effect and consider only the two water pools, much like with T_2 relaxometry. Using integrated $T_1 - T_2$ relaxometry, distinct T_1s of myelin water have been observed in frog (Does et al., 1998) and rat (Does and Gore, 2002) peripheral nerve, tissues where inter-compartmental water exchange has been found to be quite slow (Dortch et al., 2013a). However, experimentally developed models of white matter have generally suggested that water exchange results in approximately mono-exponential T_1 relaxation (Stanisz et al., 1999; Bjarnason et al., 2005). Indeed, Koenig et al. reasoned that water lifetimes in myelin to be ~60 ms and the intrinsic T_1 values of water in myelin and axons to be ~200 ms and ~2000 ms, respectively, resulting in a system that is reasonably well approximated by a fast-exchange model (Koenig et al., 1990). Likewise, the aforementioned relaxometry studies by Menon et al. demonstrated mono-exponential longitudinal relaxation in myelinated tissue, which was attributed to relatively rapid water exchange between myelin and other water (Menon et al., 1992) (see Fig 1).

Despite this widely held assumption of mono-exponential T_1, an extensive evaluation of the T_1 spectrum from human white matter has demonstrated a component with T_1 in the range of 100 to 200 ms (Labadie et al., 2014). The authors of this study note that this component is slower than the component due to MT, and they argue that myelin water lifetime is more like ≈ 260 ms, making it similar to the intrinsic T_1 of water in myelin. Thus, they proposed that the observed T_1 component is a measure of myelin water. Armed with this model, a subsequent study used a double-inversion recovery approach to selectively image this signal component (Oh et al., 2013), similar to previous myelin-selective acquisitions from nerve (Andrews et al., 2006; Travis and Does, 2005). This approach, termed the Visualization of Short Transverse relaxation time component (ViSTa), is attractive in that it requires effectively no post-acquisition signal analysis—the image intensity is proportional to the myelin water signal.

However, even if one can avoid the MT effects and it is true that myelin water lifetime is long enough to be out of the fast-exchange regime, it must still be in the intermediate exchange regime. Thus, the amplitude and T_1 of this signal component will depend not only on the myelin volume fraction but also on tissue characteristics that affect exchange and other water T_1. A recent experimental study of excised bovine brain at 37 °C and 4.7 T illuminates the picture further (Barta et al., 2015) by characterizing a four-pool model of longitudinal relaxation. This work reports observed T_1 time constants ≈ 25 ms, 60 ms, 225 ms and 1300 ms, with relative amplitudes that depend on sequence parameters. Given these data, it is possible that the 'myelin water' component observed by Labadie et al. and captured by Oh et al. is due to a combination of myelin water, myelin water exchange, and MT effects. Likely, the component is still a reasonable reporter of myelin content, but one should be careful in interpreting its amplitude as specifically proportional to myelin volume.

A third approach to characterizing neural tissue with T_1 relaxometry is to restrict the analysis to a mono-exponential model. As noted previously, a mono-exponential signal model offers tremendous advantages in terms of acquisition and signal analysis efficiency. A number of studies found correlations between mono-exponential measures of T_1 (or $R_1 = 1/T_1$) and histological estimates of myelin content (Bock et al., 2009; Bot et al., 2004; Mottershead et al., 2003; Schmierer et al., 2004, 2007, 2008; Stüber et al., 2014), so there is good empirical evidence to use this approach. In terms of modeling, the interpretation has been built off the connection between R_1 and macromolecular content. In 2007, Rooney et al. presented a fast-exchange model of R_1 equal to that of pure saline plus a linear combination of contributions from macromolecules and iron (Rooney et al., 2007). Later, a similar model was used by Callaghan et al., who noted the expected relationship between macromolecular content and myelin content (from MT studies) (Callaghan et al., 2015). Around the same time, Stüber et al. presented a similar model along with correlations to histopathological maps of phosphorus, which was interpreted as a quantitative measure of myelin content (Stüber et al., 2014). Both the Callaghan et al. and Stüber et al. studies proposed that the iron contribution to the observed R_1 could be accounted $R_2^*(= 1/T_2^*)$, thereby allowing the combination of R_1 and R_2^* measures to provide an estimate of myelin

content. (The Stüber et al. study further included a linear model of susceptibility, so the measure of any two of R_1, R_2^*, and susceptibility would be sufficient.)

Given the previous discussion of four-pool models of T_1, it might seem surprising that mono-exponential T_1 relaxometry can be effective. Unlike T_2 relaxometry though, for T_1 relaxometry (despite its added complications) a mono-exponential model can be a decent approximation. Both the Barta et al. and Labadie et al. data, as well as in vivo qMT studies (Dortch et al., 2011, 2013b; Gochberg and Gore, 2007), suggest that the fast-relaxing signals (~5–10% of the total amplitude) have T_1 ~ 10× faster than the dominant long-lived component. Hence, if these fast-relaxing signals (be they from MT, myelin water, or both), can be mostly avoided, the mono-exponential model is a good approximation. This can be achieved at 3 T using an inversion-recovery measurement with delay times $\gtrsim$ 150 ms (Rioux et al., 2015), although a bias in the estimated T_1 may remain for sequences involving short-TR gradient echo acquisitions (Ou and Gochberg, 2008), including MP2RAGE (Marques et al., 2010; Rioux et al., 2015). Also, despite the aforementioned estimates otherwise, most studies suggest that myelin water lifetimes are closer to the fast- than the slow-exchange regime for T_1 (Barta et al., 2015; Bjarnason et al., 2005; Dortch et al., 2013a; Harkins et al., 2012; Harrison et al., 1995; Koenig et al., 1990; Menon et al., 1992; Stanisz et al., 1999; Whittall et al., 1997), in which case the observed R_1 will depend approximately linearly with myelin water content. The limits of this approximation may be reflected in the observation that in spinal cord and possibly in brain, R_1 correlates with axon diameters, independently of variation in myelin content (Harkins et al., 2016), and this effect may play a role in recent observations of T_1 dependence between white matter fibre bundles (De Santis et al., 2016). Regardless, as approximations go, the use of a simple mono-exponential T_1 measurement to report on myelin content has practical value.

4.2. Acquisition Methods

An important consequence of adopting a mono-exponential model of T_1 relaxometry, in comparison to the multi-exponential models often used for T_2 and T_2^*, is that the analysis is not especially SNR limited. In turn, this means that the acquisitions can aim to be fast and relatively high resolution. The literature on T_1 mapping methods is extensive, much of which is not directly relevant to characterizing brain tissue microstructure, and so only a brief overview of the methods is provided here. For a more comprehensive report on T_1 relaxometry acquisition methods, still within the scope of brain imaging, the reader is directed to a recent review article (Lutti et al., 2014) and a report on experimental evaluations of common methods (Stikov et al., 2014).

The inversion-recovery sequence provides high sensitivity to T_1 with relatively little dependence on B_1^+ (by either including inversion flip angle in the signal model or using an adiabatic inversion pulse). However, this method is slow, and so researchers have sought faster approaches that do not compromise accuracy. One approach is the Look-Locker method (Look and Locker, 1970), which is essentially the inversion-recovery counterpart to the CPMG sequence, providing samples at multiple time points for each excitation. This approach has been combined with various fast imaging approaches (Deichmann and Haase,

1992; Gowland and Mansfield, 1993) and extended to volumetric coverage (Henderson et al., 1999; Deichmann, 2005). Another approach is the variable-flip-angle spoiled gradient echo acquisition, popularized as the method DESPOT1 (Deoni et al., 2003, 2005), which is inherently fast and readily applied as a 3D protocol. This approach requires an accurate independent accounting of B_1^+ (Deoni, 2007; Helms et al., 2008), although a recent experimental study indicates that this can be effectively implemented at 3.0 T with a standard product B_1^+ mapping method (Boudreau et al., 2017).

An interesting addendum to the use of mono-exponential T_1 relaxometry as a marker for myelin is the direct use of T_1-weighted contrast to map 'myeloarchitecture' in the cortex. To the extent that a relaxometry measure can be reduced to a scalar quantity, it makes sense that it may be effectively replaced by a normalized map of relaxation contrast. For example, rather than estimating T_1 by two images with different T_1-weighting, an alternative is to generate one image with T_1 contrast and normalize its signal intensity to a proton density weighted image. This approach has been used recently for quantitative myelin mapping (Bock et al., 2009, 2013; Oakden et al., 2017), as has a similar approach using ratio of T_1 and T_2 weighted images (Glasser and Van Essen, 2011). Further reading on these and related methods can be found in this review article (Glasser et al., 2014).

5. Conclusions

There is no denying the appeal, but the search for simple and effective ways to utilize relaxometry is an ongoing processes. T_2 relaxometry is well established as a measure of myelin content (MWF) although it is also well accepted now that MWF values may be influenced by inter-compartmental water exchange, so care should be taken when interpreting their change over time or differences between regions or subjects. The flip side to this story though is that the full T_2 spectrum likely contains more information about the microstructure of myelinated tissues, and T_2 relaxometry can provide complementary information that may help unravel the micro-structural basis for other MRI contrast, diffusion, in particular. Further experimental studies are needed to investigate this potential. The long-standing challenges to acquiring suitable multiple spin echo data have largely been overcome, but the SNR barriers to inverting a measured signal into a sum of exponentials remains and likely represents the ultimate barrier to development of MRI relaxometry. Recently, T_2^* has proven to be a viable alternative to measure MWF, but it remains to be seen whether the benefits associated with gradient echo over spin echo imaging will outweigh the additional complications of MET_2^* vs MET_2 signal analysis. Lastly, mono-exponential T_1 relaxometry seems to have found a sweet spot between the costs and benefits of a simplified model. Although this approach does not have the potential richness of information available to T_2 relaxometry, it appears to offer a reasonably simple and robust approach to probing myelination differences across the brain.

Acknowledgments

Thanks for helpful feedback from Drs Elizabeth A. Louie, Kevin D. Harkins, and Daniel F. Gochberg.

Appendix

Relaxation in a Multi-Compartment System with Exchange

For a system of J exchanging and relaxing compartments of magnetization, the rate of change of magnetization can be expressed as a set of coupled ordinary differential equations, commonly known as the Bloch-McConnell equations (McConnell, 1958; Zimmerman and Brittin, 1957). Using matrix algebra notation (Dortch et al., 2009a; Kimmich, 1997), these equations for transverse magnetization are,

$$\frac{d\mathbf{M}_{\perp}(t)}{dt} = \mathbf{L}_2\mathbf{M}_{\perp}(t), \quad \text{(A1)}$$

where $\mathbf{M}_{\perp}(t)$ is a column vector of transverse magnetizations for each compartment,

$$\mathbf{M}_{\perp}(t) = [M_{\perp,1}(t), M_{\perp,2}(t), \ldots, M_{\perp,J}(t)]^{\mathrm{T}},$$

and $\mathbf{L}_2$ contains the compartmental relaxation and exchange rate constants,

$$\mathbf{L}_2 = \begin{pmatrix} -R_{2,1} & & & \\ & -R_{2,2} & & \\ & & \ddots & \\ & & & -R_{2,J} \end{pmatrix} + \begin{pmatrix} -\sum_{i\neq 1} k_{1,i} & k_{2,1} & k_{3,1} & \cdots & k_{J,1} \\ k_{1,2} & -\sum_{i\neq 2} k_{2,i} & k_{3,2} & \cdots & k_{J,2} \\ \vdots & & \ddots & & \vdots \\ k_{1,J} & & \cdots & & -\sum_{i\neq J} k_{J,i} \end{pmatrix}.$$

Here, $R_{2,j}$ is the transverse relaxation rate constant in the j^{th} compartment, and $k_{i,j}$ is the first-order exchange rate constant from the i^{th} to the j^{th} compartments. Note that $k_{i,j}M_{0,i} = k_{j,i}M_{0,j}$, and magnetization lifetimes in compartment j can be defined as $\tau_j = 1/\Sigma_{i\neq j} k_{j,i}$.

Equation (A1) solves to

$$\mathbf{M}_{\perp}(t) = \exp(\mathbf{L}_2 t)\mathbf{M}_{\perp}(0), \quad \text{(A2)}$$

which can be expressed in terms of the eigenvalues, λ_i, $i = 1$ to J, and the matrix of eigenvectors, $\mathbf{U}$, of $\mathbf{L}_2$ as,

$$\mathbf{M}_{\perp}(t) = \mathbf{U}\begin{pmatrix} \exp(\lambda_1 t) & & \\ & \ddots & \\ & & \exp(\lambda_J t) \end{pmatrix}\mathbf{U}^{-1}\mathbf{M}_{\perp}(0). \quad \text{(A3)}$$

Thus, the negative eigenvalues of $\mathbf{L}_2$ are the observed relaxation rates. The observed signal is the sum of the elements of $\mathbf{M}_{\perp}(t)$; therefore, equation (A3) provides a simple way to compute the observed transverse magnetization from a given multi-compartment system,

with exchange. Similar equations can be worked out for longitudinal relaxation and sequences of arbitrary complexity. Examples can be found in the following literature (Dortch et al., 2009b, 2013a; Kimmich, 1997; Spencer and Fishbein, 2000).

References

Akhondi-Asl A, Afacan O, Balasubramanian M, Mulkern RV, Warfield SK. Fast myelin water fraction estimation using 2D multislice CPMG. Magn Reson Med. 2015; 76(4):1301–1313. [PubMed: 26536382]

Alonso-Ortiz E, Levesque IR, Paquin R, Pike GB. Field inhomogeneity correction for gradient echo myelin water fraction imaging. Magn Reson Med. 2017a; 78(1):49–57. [PubMed: 27416957]

Alonso-Ortiz E, Levesque IR, Pike GB. MRI-based myelin water imaging: A technical review. Magn Reson Med. 2015; 73(1):70–81. [PubMed: 24604728]

Alonso-Ortiz E, Levesque IR, Pike GB. Impact of magnetic susceptibility anisotropy at 3 T and 7 T on T2*-based myelin water fraction imaging. Neuroimage. 2017b. URL

Alonso-Ortiz E, Levesque IR, Pike GB. Multi-gradient-echo myelin water fraction imaging: Comparison to the multi-echo-spin-echo technique. Magn Reson Med. 2017c. URL

Andrews TJ, Osborne MT, Does MD. Diffusion of myelin water. Magn Reson Med. 2006; 56(2):381–385. [PubMed: 16767712]

Barker GJ, Mareci TH. Suppression of artifacts in multiple-echo magnetic resonance. J Magn Reson. 1989; 83(1):11–28.

Barta R, Kalantari S, Laule C, Vavasour IM, MacKay AL, Michal CA. Modeling T1 and T2 relaxation in bovine white matter. J Magn Reson. 2015; 259:56–67. [PubMed: 26295169]

Beaulieu C, Fenrich FR, Allen PS. Multicomponent water proton transverse relaxation and T2-discriminated water diffusion in myelinated and nonmyelinated nerve. Magn Reson Imaging. 1998; 16(10):1201–10. [PubMed: 9858277]

Ben-Eliezer N, Sodickson DK, Block KT. Rapid and accurate T2 mapping from multi-spin-echo data using Bloch-simulation-based reconstruction. Magn Reson Med. 2015; 73(2):809–17. [PubMed: 24648387]

Bertero M, Brianzi P, Pike ER. On the recovery and resolution of exponential relaxational rates from experimental data: Laplace transform inversions in weighted spaces. Inverse Probl. 1985; 1:1–15.

Bieri O, Scheffler K. On the origin of apparent low tissue signals in balanced SSFP. Magn Reson Med. 2006; 56(5):1067–1074. [PubMed: 17036284]

Bjarnason TA, McCreary CR, Dunn JF, Mitchell JR. Quantitative T2 analysis: The effects of noise, regularization, and multivoxel approaches. Magn Reson Med. 2009; 24(1):212–217.

Bjarnason TA, Vavasour IM, Chia CLL, MacKay AL. Characterization of the NMR behavior of white matter in bovine brain. Magn Reson Med. 2005; 54(5):1072–1081. [PubMed: 16200557]

Bock NA, Hashim E, Janik R, Konyer NB, Weiss M, Stanisz GJ, Turner R, Geyer S. Optimizing T1-weighted imaging of cortical myelin content at 3.0T. Neuroimage. 2013; 65:1–12. [PubMed: 23036446]

Bock NA, Kocharyan A, Liu JV, Silva AC. Visualizing the entire cortical myelination pattern in marmosets with magnetic resonance imaging. J Neurosci Meth. 2009; 185(1):15–22.

Bonilla I, Snyder RE. Transverse relaxation in rat optic nerve. NMR Biomed. 2007; 20(2):113–120. [PubMed: 16998953]

Borgia GC, Brown RJS, Fantazzini P. Uniform-Penalty Inversion of Multiexponential Decay Data. J Magn Reson. 1998; 132(1):65–77. [PubMed: 9615412]

Borgia GC, Brown RJS, Fantazzini P. Uniform-Penalty Inversion of Multiexponential Decay Data. J Magn Reson. 2000; 147(2):273–285. [PubMed: 11097819]

Bot JCJ, Blezer ELA, Kamphorst W, Lycklama A, Nijeholt GJ, Ader HJ, Castelijns JA, Ig KN, Bergers E, Ravid R, Polman C, Barkhof F. The spinal cord in multiple sclerosis: relationship of high-spatial-resolution quantitative MR imaging findings to histopathologic results. Radiology. 2004; 233(2):531–540. [PubMed: 15385682]

Boudreau M, Tardif CL, Stikov N, Sled JG, Lee W, Pike GB. B1 mapping for bias-correction in quantitative T1 imaging of the brain at 3T using standard pulse sequences. J Magn Reson Imag. 2017; 74(Pt 2):634–10.

Bouhrara M, Reiter DA, Celik H, Fishbein KW, Kijowski R, Spencer RG. Analysis of mcDESPOT- and CPMG-derived parameter estimates for two-component nonexchanging systems. Magn Reson Med. 2016; 75(6):2406–2420. [PubMed: 26140371]

Bouhrara M, Spencer RG. Improved determination of the myelin water fraction in human brain using magnetic resonance imaging through Bayesian analysis of mcDESPOT. Neuroimage. 2016; 127(C):456–471. [PubMed: 26499810]

Bouhrara M, Spencer RG. Rapid simultaneous high-resolution mapping of myelin water fraction and relaxation times in human brain using BMC-mcDESPOT. Neuroimage. 2017; 147:800–811. [PubMed: 27729276]

Brownstein KR, Tarr CE. Importance of classical diffusion in NMR studies of water in biological cells. Phys Rev A. 1979; 19(6):2446–2453.

Callaghan MF, Helms G, Lutti A, Mohammadi S, Weiskopf N. A general linear relaxometry model of R1 using imaging data. Magn Reson Med. 2015; 73(3):1309–1314. [PubMed: 24700606]

Carr HY, Purcell EM. Effects of diffusion on free precession in nuclear magnetic resonance experiments. Phys Rev. 1954; 94(3):630–638.

Crawley AP, Henkelman RM. Errors in T2 estimation using multislice multiple-echo imaging. Magn Reson Med. 1987; 4(1):34–47. [PubMed: 3821477]

Crooijmans HJA, Gloor M, Bieri O, Scheffler K. Influence of MT effects on T2 quantification with 3D balanced steady-state free precession imaging. Magn Reson Med. 2011; 65(1):195–201. [PubMed: 20981754]

De Santis S, Barazany D, Jones DK, Assaf Y. Resolving relaxometry and diffusion properties within the same voxel in the presence of crossing fibres by combining inversion recovery and diffusion-weighted acquisitions. Magn Reson Med. 2016; 75(1):372–380. [PubMed: 25735538]

Deichmann R. Fast high-resolution T1 mapping of the human brain. Magn Reson Med. 2005; 54(1): 20–27. [PubMed: 15968665]

Deichmann R, Haase A. Quantification of T1 values by SNAPSHOT-FLASH NMR imaging. J Magn Reson. 1992; 96:608–612.

Deoni SC, Rutt BK, Arun T, Pierpaoli C, Jones DK. Gleaning multicomponent T1 and T2 information from steady-state imaging data. Magn Reson Med. 2008; 60(6):1372–1387. [PubMed: 19025904]

Deoni SC, Rutt BK, Peters TM. Rapid combined T1 and T2 mapping using gradient recalled acquisition in the steady state. Magn Reson Med. 2003; 49(3):515–526. [PubMed: 12594755]

Deoni SCL. High-resolution T1 mapping of the brain at 3T with driven equilibrium single pulse observation of T1 with high-speed incorporation of RF field inhomogeneities (DESPOT1-HIFI). J Magn Reson Imaging. 2007; 26(4):1106–1111. [PubMed: 17896356]

Deoni SCL, Peters TM, Rutt BK. High-resolution T1 and T2 mapping of the brain in a clinically acceptable time with DESPOT1 and DESPOT2. Magn Reson Med. 2005; 53(1):237–241. [PubMed: 15690526]

Does M, Gore J. Complications of nonlinear echo time spacing for measurement of T-2. NMR Biomed. 2000a; 13(1):1–7. [PubMed: 10668048]

Does M, Gore J. Compartmental study of T-1 and T-2 in rat brain and trigeminal nerve in vivo. Magn Reson Med. 2002; 47(2):274–283. [PubMed: 11810670]

Does M, Snyder R. Multiexponential T-2 relaxation in degenerating peripheral nerve. Magn Reson Med. 1996; 35(2):207–213. [PubMed: 8622585]

Does MD, Beaulieu C, Allen PS, Snyder RE. Multi-component T1 relaxation and magnetisation transfer in peripheral nerve. Magn Reson Imaging. 1998; 16(9):1033–1041. [PubMed: 9839987]

Does MD, Gore JC. Rapid acquisition transverse relaxometric imaging. J Magn Reson. 2000b; 147(1): 116–20. [PubMed: 11042054]

Does MD, Snyder RE. Multiecho imaging with suboptimal spoiler gradients. J Magn Reson. 1998; 131(1):25–31. [PubMed: 9533902]

Dortch RD, Harkins KD, Juttukonda MR, Gore JC, Does MD. Characterizing inter-compartmental water exchange in myelinated tissue using relaxation exchange spectroscopy. Magn Reson Med. 2013a; 70(5):1450–1459. [PubMed: 23233414]

Dortch RD, Horch RA, Does MD. Development, simulation, and validation of NMR relaxation-based exchange measurements. J Chem Phys. 2009a; 131(16):164502. [PubMed: 19894951]

Dortch RD, Li K, Gochberg DF, Welch EB, Dula AN, Tamhane AA, Gore JC, Smith SA. Quantitative magnetization transfer imaging in human brain at 3 t via selective inversion recovery. Magn Reson Med. 2011; 66(5):1346–1352. [PubMed: 21608030]

Dortch RD, Moore J, Li K, Jankiewicz M, Gochberg DF, Hirtle JA, Gore JC, Smith SA. Quantitative magnetization transfer imaging of human brain at 7T. Neuroimage. 2013b; 64:640–649. [PubMed: 22940589]

Dortch RD, Yankeelov TE, Yue Z, Quarles CC, Gore JC, Does MD. Evidence of multiexponential T2 in rat glioblastoma. NMR Biomed. 2009b; 22(6):609–618. [PubMed: 19267385]

Du YP, Chu R, Hwang D, Brown MS, Kleinschmidt-DeMasters BK, Singel D, Simon JH. Fast multislice mapping of the myelin water fraction using multicompartment analysis of T2* decay at 3T: a preliminary postmortem study. Magn Reson Med. 2007; 58(5):865–70. [PubMed: 17969125]

Dula AN, Gochberg DF, Valentine HL, Valentine WM, Does MD. Multiexponential T2, magnetization transfer, and quantitative histology in white matter tracts of rat spinal cord. Magn Reson Med. 2010; 63(4):902–909. [PubMed: 20373391]

Duyn JH. Studying brain microstructure with magnetic susceptibility contrast at high-field; Neuroimage. 2017. 1–10. URL

Edzes HT, Samulski ET. The measurement of cross-relaxation effects in the proton NMR spin-lattice relaxation of water in biological systems: Hydrated collagen and muscle. J Magn Reson. 1978; 31(2):207–229.

Fenrich FR. Master's thesis. Univerversity of Alberta: 1992. A simulation and experimental study of water proton relaxation in a white matter model.

Fenrich FR, Beaulieu C, Allen PS. Relaxation times and microstructures. NMR Biomed. 2001; 14(2): 133–9. [PubMed: 11320538]

Fischer HW, Rinck PA, Van Haverbeke Y, Muller RN. Nuclear relaxation of human brain gray and white matter: analysis of field dependence and implications for MRI. Magn Reson Med. 1990; 16(2):317–334. [PubMed: 2266850]

Gareau PJ, Rutt BK, Bowen CV, Karlik SJ, Mitchell JR. In vivo measurements of multi-component T2 relaxation behaviour in guinea pig brain. Magn Reson Imaging. 1999; 17(9):1319–1325. [PubMed: 10576717]

Glasser MF, Goyal MS, Preuss TM, Raichle ME, Van Essen DC. Trends and properties of human cerebral cortex: Correlations with cortical myelin content. Neuroimage. 2014; 93(Part 2):165–175. [PubMed: 23567887]

Glasser MF, Van Essen DC. Mapping Human Cortical Areas In Vivo Based on Myelin Content as Revealed by T1- and T2-Weighted MRI. J Neurosci. 2011; 31(32):11597–11616. [PubMed: 21832190]

Gloor M, Scheffler K, Bieri O. Quantitative magnetization transfer imaging using balanced SSFP. Magn Reson Med. 2008; 60(3):691–700. [PubMed: 18727085]

Go KG, Edzes HT. Water in brain edema. Observations by the pulsed nuclear magnetic resonance technique. Arch Neurol. 1975; 32(7):462–465. [PubMed: 1137512]

Gochberg DF, Gore JC. Quantitative imaging of magnetization transfer using an inversion recovery sequence. Magn Reson Med. 2003; 49(3):501–505. [PubMed: 12594753]

Gochberg DF, Gore JC. Quantitative magnetization transfer imaging via selective inversion recovery with short repetition times. Magn Reson Med. 2007; 57(2):437–441. [PubMed: 17260381]

Gochberg DF, Kennan RP, Gore JC. Quantitative studies of magnetization transfer by selective excitation and T1 recovery. Magn Reson Med. 1997; 38(2):224–231. [PubMed: 9256101]

Gochberg DF, Kennan RP, Robson MD, Gore JC. Quantitative imaging of magnetization transfer using multiple selective pulses. Magn Reson Med. 1999; 41(5):1065–1072. [PubMed: 10332891]

Gowland P, Mansfield P. Accurate measurement of T1 in vivo in less than 3 seconds using echo-planar imaging. Magn Reson Med. 1993; 30(3):351–354. [PubMed: 8412607]

Graham SJ, Stanchev PL, Bronskill MJ. Criteria for analysis of multicomponent tissue T2 relaxation data. Magn Reson Med. 1996; 35(3):370–378. [PubMed: 8699949]

Harkins KD, Dula AN, Does MD. Effect of intercompartmental water exchange on the apparent myelin water fraction in multiexponential T2 measurements of rat spinal cord. Magn Reson Med. 2012; 67(3):793–800. [PubMed: 21713984]

Harkins KD, jJunzhong X, Dula AN, Li K, Valentine WM, Gochberg DF, Gore JC, Does MD. The microstructural correlates of T1 in white matter. Magn Reson Med. 2016; 75(3):1341–1345. [PubMed: 25920491]

Harrison R, Bronskill MJ, Mark Henkelman R. Magnetization Transfer and T2 Relaxation Components in Tissue. Magn Reson Med. 1995; 33(4):490–496. [PubMed: 7776879]

Helms G, Dathe H, Dechent P. Quantitative FLASH MRI at 3T using a rational approximation of the Ernst equation. Magn Reson Med. 2008; 59(3):667–672. [PubMed: 18306368]

Henderson E, McKinnon G, Lee TY, Rutt BK. A fast 3D Look-Locker method for volumetric T1 mapping. Magn Reson Imaging. 1999; 17(8):1163–1171. [PubMed: 10499678]

Hennig J. Multiecho imaging sequences with low refocusing flip angles. J Magn Reson. 1988; 78(3): 397–407.

Huang C, Bilgin A, Barr T, Altbach MI. T2 relaxometry with indirect echo compensation from highly undersampled data. Magn Reson Med. 2013; 70(4):1026–1037. [PubMed: 23165796]

Hwang D, Chung H, Nam Y, Du YP, Jang U. Robust mapping of the myelin water fraction in the presence of noise: Synergic combination of anisotropic diffusion filter and spatially regularized nonnegative least squares algorithm. J Magn Reson Imaging. 2011; 34(1):189–195. [PubMed: 21618330]

Hwang D, Kim D-H, Du YP. In vivo multi-slice mapping of myelin water content using T2* decay. Neuroimage. 2010; 52(1):198–204. [PubMed: 20398770]

Istratov AA, Vyvenko OF. Exponential analysis in physical phenomena. Rev Sci Instrum. 1999; 70(2): 1233–1257.

Jolesz FA, Polak JF, Adams DF, Ruenzel PW. Myelinated and nonmyelinated nerves: comparison of proton MR properties. Radiology. 1987; 164(1):89–91. [PubMed: 3035608]

Jolesz FA, Polak JF, Ruenzel PW, Adams DF. Wallerian degeneration demonstrated by magnetic resonance: spectroscopic measurements on peripheral nerve. Radiology. 1984; 152(1):85–87. [PubMed: 6729140]

Jones C, xiang Q, Whittall KP, MacKay AL. Proceedings of the ISMRM. Toronto: 2003a. Calculating T2 and B1 from decay curves collected with non-180 refocusing pulses; 1018

Jones CK, Whittall KP, Mackay AL. Robust myelin water quantification: averaging vs. spatial filtering. Magn Reson Med. 2003b; 50(1):206–209. [PubMed: 12815697]

Jones CK, Xiang Q-S, Whittall KP, Mackay AL. Linear combination of multiecho data: short T2 component selection. Magn Reson Med. 2004; 51(3):495–502. [PubMed: 15004790]

Kay S, Eldar YC. Rethinking biased estimation. IEEE Signal Proc Mag. 2008; 25(3):133–136.

Kimmich R. NMR: tomography, diffusometry, relaxometry. Springer-Verlag; Berlin: 1997.

Koenig SH, Brown RD, Spiller M, Lundbom N. Relaxometry of brain: Why white matter appears bright in MRI. Magn Reson Med. 1990; 14(3):482–495. [PubMed: 2355830]

Kolind SH, Laule C, Vavasour IM, Li DK, Traboulsee AL, Mädler B, Moore GW, MacKay AL. Complementary information from multi-exponential T2 relaxation and diffusion tensor imaging reveals differences between multiple sclerosis lesions. Neuroimage. 2008; 40(1):77–85. [PubMed: 18226549]

Kolind SH, Mädler B, Fischer S, Li DKB, Mackay AL. Myelin water imaging: Implementation and development at 3.0T and comparison to 1.5T measurements. Magn Reson Med. 2009; 62(1):106–115. [PubMed: 19353659]

Kozlowski P, Liu J, Yung AC, Tetzlaff W. High-resolution myelin water measurements in rat spinal cord. Magn Reson Med. 2008; 59(4):796–802. [PubMed: 18302247]

Kroeker RM, Henkelman RM. Analysis of biological NMR relaxation data with continuous distributions of relaxation times. J Magn Reson. 1986; 69(2):218–235.

Kwon, Oh In WooEung JeDu Yiping P, Hwang Dosik. A tissue-relaxation-dependent neighboring method for robust mapping of the myelin water fraction. Neuroimage. 2010; 74:12–21.

Labadie C, Lee J-H, Rooney WD, Jarchow S, Aubert-Frécon M, Springer CS, Möller HE. Myelin water mapping by spatially regularized longitudinal relaxographic imaging at high magnetic fields. Magn Reson Med. 2014; 71(1):375–387. [PubMed: 23468414]

Lancaster JL, Andrews T, Hardies LJ, Dodd S, Fox PT. Three-pool model of white matter. J Magn Reson Imaging. 2002; 17(1):1–10.

Lang DJM, Yip E, MacKay AL, Thornton AE, Vila-Rodriguez F, MacEwan GW, Kopala LC, Smith GN, Laule C, MacRae CB, Honer WG. 48 echo T2 myelin imaging of white matter in first-episode schizophrenia: evidence for aberrant myelination. NeuroImage-Clin. 2014; 6:408–414. [PubMed: 25379454]

Lankford CL, Does MD. On the inherent precision of mcDESPOT. Magn Reson Med. 2013; 69(1): 127–136. [PubMed: 22411784]

Lankford CL, Does MD. Propagation of error from parameter constraints in quantitative MRI: Example application of multiple spin echo T2 mapping. Magn Reson Med. 2017. URL

Lankford CL, Dortch RD, Does MD. Fast T2 mapping with multiple echo, aesar cipher acquisition and model-based reconstruction. Magn Reson Med. 2015; 73(3):1065–1074. [PubMed: 24753216]

Laule C, Kolind SH, Bjarnason TA, Li DKB, MacKay AL. In vivo multiecho T2 relaxation measurements using variable TR to decrease scan time. Magn Reson Imaging. 2007a; 25(6):834–839. [PubMed: 17482413]

Laule C, Kozlowski P, Leung E, Li DKB, Mackay AL, Moore GRW. Myelin water imaging of multiple sclerosis at 7 T: correlations with histopathology. Neuroimage. 2008; 40(4):1575–1580. [PubMed: 18321730]

Laule C, Leung E, Li DK, Traboulsee AL, Paty DW, MacKay AL, Moore GR. Myelin water imaging in multiple sclerosis: quantitative correlations with histopathology. Mult Scler. 2006; 12(6):747–753. [PubMed: 17263002]

Laule C, Vavasour I, Zhao Y, Traboulsee A, Oger J, Vavasour J, Mackay A, Li D. Two-year study of cervical cord volume and myelin water in primary progressive multiple sclerosis. Mult Scler J. 2010; 16(6):670–677.

Laule C, Vavasour IM, Kolind SH, Traboulsee AL, Moore GRW, Li DKB, Mackay AL. Long T2 water in multiple sclerosis: what else can we learn from multi-echo T2 relaxation? J Neurol. 2007b; 254(11):1579–1587. [PubMed: 17762945]

Laule C, Vavasour IM, Mädler B, Kolind SH, Sirrs SM, Brief EE, Traboulsee AL, Moore GRW, Li DKB, Mackay AL. MR evidence of long T2 water in pathological white matter. J Magn Reson Imaging. 2007c; 26(4):1117–1121. [PubMed: 17896375]

Laule C, Vavasour IM, Moore GRW, Oger J, Li DKB, Paty DW, MacKay AL. Water content and myelin water fraction in multiple sclerosis. A T2 relaxation study. J Neurol. 2004; 251(3):284–293. [PubMed: 15015007]

Laule C, Yung A, Pavolva V, Bohnet B, Kozlowski P, Hashimoto SA, Yip S, Li DK, Moore GW. High-resolution myelin water imaging in post-mortem multiple sclerosis spinal cord: A case report. Mult Scler J. 2016; 22(11):1485–1489.

Lawson CL, Hanson RJ. Classics in Applied Mathematics. SIAM; 1995. Solving least squares problems.

Lebel RM, Wilman AH. Transverse relaxometry with stimulated echo compensation. Magn Reson Med. 2010; 64(4):1005–1014. [PubMed: 20564587]

Lenz C, Klarhöfer M, Scheffler K. Limitations of rapid myelin water quantification using 3D bSSFP. MAGMA. 2010; 23(3):139–151. [PubMed: 20424884]

Levesque IR, Chia CLL, Pike GB. Reproducibility of in vivo magnetic resonance imaging-based measurement of myelin water. J Magn Reson Imag. 2010; 32(1):60–68.

Levesque IR, Pike GB. Characterizing healthy and diseased white matter using quantitative magnetization transfer and multicomponent T2 relaxometry: A unified view via a four-pool model. Magn Reson Med. 2009; 62(6):1487–1496. [PubMed: 19859946]

Lin M, He H, Tong Q, Ding Q, Yan X, Feiweier T, Zhong J. Effect of myelin water exchange on DTI-derived parameters in diffusion MRI: Elucidation of TE dependence. Magn Reson Med. 2017; 66:259–11.

Look DC, Locker DR. Time saving in measurement of NMR and EPR relaxation times. Rev Sci Instrum. 1970; 41(2):250–251.

Lukzen NN, Petrova MV, Koptyug IV, Savelov AA, Sagdeev RZ. The generating functions formalism for the analysis of spin response to the periodic trains of rf pulses. echo sequences with arbitrary refocusing angles and resonance offsets. J Magn Reson. 2009; 196(2):164–9. [PubMed: 19091610]

Lutti A, Dick F, Sereno MI, Weiskopf N. Using high-resolution quantitative mapping of R1 as an index of cortical myelination. Neuroimage. 2014; 93(2):176–188. [PubMed: 23756203]

Ma D, Gulani V, Seiberlich N, Liu K, Sunshine JL, Duerk JL, Griswold MA. Magnetic resonance fingerprinting. Nature. 2013; 495(7440):187–192. [PubMed: 23486058]

MacKay A, Whittall K, Adler J, Li D, Paty D, Graeb D. In-Vivo Visualization of Myelin Water in Brain by Magnetic-Resonance. Magn Reson Med. 1994; 31(6):673–677. [PubMed: 8057820]

Mädler B, Drabycz SA, Kolind SH, Whittall KP, MacKay AL. Is diffusion anisotropy an accurate monitor of myelination? Correlation of multicomponent T2 relaxation and diffusion tensor anisotropy in human brain. Magn Reson Imaging. 2008; 26(7):874–888. [PubMed: 18524521]

Majumdar S, Gmitro A, Orphanoudakis SC, Reddy D, Gore JC. An estimation and correction scheme for system imperfections in multiple-echo magnetic resonance imaging. Magn Reson Med. 1987; 4(3):203–220. [PubMed: 3574056]

Majumdar S, Orphanoudakis SC, Gmitro A, O'Donnell M, Gore JC. Errors in the measurements of T2 using multiple-echo MRI techniques. I. Effects of radiofrequency pulse imperfections. Magn Reson Med. 1986a; 3(3):397–417. [PubMed: 3724419]

Majumdar S, Orphanoudakis SC, Gmitro A, O'Donnell M, Gore JC. Errors in the measurements of T2 using multiple-echo MRI techniques. II. Effects of static field inhomogeneity. Magn Reson Med. 1986b; 3(4):562–574. [PubMed: 3747818]

Marques JP, Kober T, Krueger G, van der Zwaag W, Van de Moortele P-F, Gruetter R. MP2RAGE, a self bias-field corrected sequence for improved segmentation and T1-mapping at high field. Neuroimage. 2010; 49(2):1271–1281. [PubMed: 19819338]

McConnell HM. Reaction Rates by Nuclear Magnetic Resonance. J Chem Phys. 1958; 28(3):430.

McCreary CR, Bjarnason TA, Skihar V, Mitchell JR, Yong VW, Dunn JF. Multiexponential T2 and magnetization transfer MRI of demyelination and remyelination in murine spinal cord. Neuroimage. 2009; 45(4):1173–1182. [PubMed: 19349232]

McPhee KC, Wilman AH. Transverse relaxation and flip angle mapping: Evaluation of simultaneous and independent methods using multiple spin echoes. Magn Reson Med. 2017; 77(5):2057–2065. [PubMed: 27367906]

Meiboom S, Gill D. Modified Spin-Echo Method for Measuring Nuclear Relaxation Times. Rev Sci Instrum. 1958; 29:688–691.

Menon RS, Allen PS. Application of continuous relaxation time distributions to the fitting of data from model systems and excised tissue. Magn Reson Med. 1991; 20(2):214–227. [PubMed: 1775048]

Menon RS, Rusinko MS, Allen PS. Proton relaxation studies of water compartmentalization in a model neurological system. Magn Reson Med. 1992; 28(2):264–274. [PubMed: 1281258]

Meyers SM, Vavasour IM, Mädler B, Harris T, Fu E, Li DKB, Traboulsee AL, Mackay AL, Laule C. Multicenter measurements of myelin water fraction and geometric mean T2 : intra- and intersite reproducibility. J Magn Reson Imaging. 2013; 38(6):1445–1453. [PubMed: 23553991]

Moore GR, Leung E, MacKay AL, Vavasour IM, Whittall KP, Cover KS, Li DK, Hashimoto SA, Oger J, Sprinkle TJ, Paty DW. A pathology-MRI study of the short-T2 component in formalin-fixed multiple sclerosis brain. Neurology. 2000; 55(10):1506–1510. [PubMed: 11094105]

Moore GRW, Laule C. Neuropathologic correlates of magnetic resonance imaging in multiple sclerosis. J Neuropath Exp Neur. 2012; 71(9):762–778. [PubMed: 22892523]

Mottershead JP, Schmierer K, Clemence M, Thornton JS, Scaravilli F, Barker GJ, Tofts PS, Newcombe J, Cuzner ML, Ordidge RJ, McDonald WI, Miller DH. High field MRI correlates of myelin

content and axonal density in multiple sclerosis. J Neurol. 2003; 250(11):1293–1301. [PubMed: 14648144]

Nam Y, Lee J, Hwang D, Kim D-H. Improved estimation of myelin water fraction using complex model fitting. Neuroimage. 2015; 116:214–21. [PubMed: 25858448]

Nguyen TD, Deh K, Monohan E, Pandya S, Spincemaille P, Raj A, Wang Y, Gauthier SA. Feasibility and reproducibility of whole brain myelin water mapping in 4 minutes using fast acquisition with spiral trajectory and adiabatic T2prep (FAST-T2) at 3T. Magn Reson Med. 2016; 76(2):456–465. [PubMed: 26331978]

Norton WT, Cammer W. Isolation and characterization of myelin. Myelin: Springer; 1984. 147–195.

Nunes D, Cruz TL, Jespersen SN, Shemesh N. Mapping axonal density and average diameter using non-monotonic time-dependent gradient-echo MRI. J Magn Reson. 2017; 277:117–130. [PubMed: 28282586]

Oakden W, Bock NA, Al-Ebraheem A, Farquharson MJ, Stanisz GJ. Early regional cuprizone-induced demyelination in a rat model revealed with MRI. NMR Biomed. 2017; 28(3):e3743–9.

Odrobina EE, Lam TY, Pun T, Midha R, Stanisz GJ. MR properties of excised neural tissue following experimentally induced demyelination. NMR Biomed. 2005; 18(5):277–284. [PubMed: 15948233]

Oh J, Han ET, Pelletier D, Nelson SJ. Measurement of in vivo multi-component T2 relaxation times for brain tissue using multi-slice T2 prep at 1.5 and 3 T. Magn Reson Imaging. 2006; 24(1):33–43. [PubMed: 16410176]

Oh S-H, Bilello M, Schindler M, Markowitz CE, Detre JA, Lee J. Direct visualization of short transverse relaxation time component (ViSTa). Neuroimage. 2013; 83:485–492. [PubMed: 23796545]

Ou X, Gochberg DF. MT effects and T1 quantification in single-slice spoiled gradient echo imaging. Magn Reson Med. 2008; 59(4):835–845. [PubMed: 18302249]

Peled S, Cory DG, Raymond SA, Kirschner DA, Jolesz FA. Water diffusion, T2, and compartmentation in frog sciatic nerve. Magn Reson Med. 1999; 42(5):911–8. [PubMed: 10542350]

Poon C, Henkelman R. Practical T2 Quantitation for Clinical-Applications. J Magn Reson Imaging. 1992; 2(5):541–553. [PubMed: 1392247]

Prasloski T, Mädler B, Xiang Q-S, MacKay A, Jones C. Applications of stimulated echo correction to multicomponent T2 analysis. Magn Reson Med. 2012a; 67(6):1803–1814. [PubMed: 22012743]

Prasloski T, Rauscher A, Mackay AL, Hodgson M, Vavasour IM, Laule C, Mädler B. Rapid whole cerebrum myelin water imaging using a 3D GRASE sequence. Neuroimage. 2012b; 63(1):533–539. [PubMed: 22776448]

Pun TWC, Odrobina E, Xu QG, Lam TYJ, Munro CA, Midha R, Stanisz GJ. Histological and magnetic resonance analysis of sciatic nerves in the tellurium model of neuropathy. J Peripher Nerv Syst. 2005; 10(1):38–46. [PubMed: 15703017]

Qin W, Shui Yu C, Zhang F, Du XY, Jiang H, Xia Yan Y, Cheng Li K. Effects of echo time on diffusion quantification of brain white matter at 1.5T and 3.0T. Magn Reson Med. 2009; 61(4):755–760. [PubMed: 19191286]

Raj A, Pandya S, Shen X, LoCastro E, Nguyen TD, Gauthier SA. Multi-Compartment T2 Relaxometry Using a Spatially Constrained Multi-Gaussian Model. Plos One. 2014; 9(6):e98391. [PubMed: 24896833]

Rioux JA, Levesque IR, Rutt BK. Biexponential longitudinal relaxation in white matter: Characterization and impact on T1 mapping with IR-FSE and MP2RAGE. Magn Reson Med. 2015; 75(6):2265–2277. [PubMed: 26190230]

Rooney WD, Johnson G, Li X, Cohen ER, Kim S-G, Ugurbil K, Springer CS. Magnetic field and tissue dependencies of human brain longitudinal 1H2O relaxation in vivo. Magn Reson Med. 2007; 57(2):308–318. [PubMed: 17260370]

Sati P, van Gelderen P, Silva AC, Reich DS, Merkle H, de Zwart JA, Duyn JH. Micro-compartment specific T2* relaxation in the brain. Neuroimage. 2013; 77:268–78. [PubMed: 23528924]

Schmierer K, Scaravilli F, Altmann DR, Barker GJ, Miller DH. Magnetization transfer ratio and myelin in postmortem multiple sclerosis brain. Ann Neurol. 2004; 56(3):407–415. [PubMed: 15349868]

Schmierer K, Tozer DJ, Scaravilli F, Altmann DR, Barker GJ, Tofts PS, Miller DH. Quantitative magnetization transfer imaging in postmortem multiple sclerosis brain. J Magn Reson Imaging. 2007; 26(1):41–51. [PubMed: 17659567]

Schmierer K, Wheeler Kingshott CAM, Tozer DJ, Boulby PA, Parkes HG, Yousry TA, Scaravilli F, Barker GJ, Tofts PS, Miller DH. Quantitative magnetic resonance of postmortem multiple sclerosis brain before and after fixation. Magn Reson Med. 2008; 59(2):268–277. [PubMed: 18228601]

Schmitt P, Griswold MA, Jakob PM, Kotas M, Gulani V, Flentje M, Haase A. Inversion recovery TrueFISP: Quantification of T1,T2, and spin density. Magn Reson Med. 2004; 51(4):661–667. [PubMed: 15065237]

Shrager R, Weiss G, Spencer R. Optimal time spacings for T2 measurements: monoexponential and biexponential systems. NMR Biomed. 1998; 11(6):297–305. [PubMed: 9802472]

Sirrs SM, Laule C, Mädler B, Brief EE, Tahir SA, Bishop C, Mackay AL. Normal-appearing white matter in patients with phenylketonuria: water content, myelin water fraction, and metabolite concentrations. Radiology. 2007; 242(1):236–243. [PubMed: 17185670]

Sled JG. Modelling and interpretation of magnetization transfer imaging in the brain. Neuroimage. 2017. URL

Sled JG, Levesque I, Santos AC, Francis SJ, Narayanan S, Brass SD, Arnold DL, Pike GB. Regional variations in normal brain shown by quantitative magnetization transfer imaging. Magn Reson Med. 2004; 51(2):299–303. [PubMed: 14755655]

Spencer RG, Fishbein KW. Measurement of Spin–Lattice Relaxation Times and Concentrations in Systems with Chemical Exchange Using the One-Pulse Sequence: Breakdown of the Ernst Model for Partial Saturation in Nuclear Magnetic Resonance Spectroscopy. J Magn Reson. 2000; 142(1):120–135. [PubMed: 10617442]

Stanisz G, Henkelman R. Diffusional anisotropy of T-2 components in bovine optic nerve. Magn Reson Med. 1998; 40(3):405–410. [PubMed: 9727943]

Stanisz GJ, Kecojevic A, Bronskill MJ, Henkelman RM. Characterizing white matter with magnetization transfer and T(2). Magn Reson Med. 1999; 42(6):1128–1136. [PubMed: 10571935]

Stanisz GJ, Midha R, Munro CA, Henkelman RM. MR properties of rat sciatic nerve following trauma. Magn Reson Med. 2001; 45(3):415–420. [PubMed: 11241698]

Stanisz GJ, Webb S, Munro CA, Pun T, Midha R. MR properties of excised neural tissue following experimentally induced inflammation. Magn Reson Med. 2004; 51(3):473–479. [PubMed: 15004787]

Stewart WA, Mackay AL, Whittall KP, Moore GRW, Paty DW. Spin-spin relaxation in experimental allergic Encephalomyelitis. Analysis of CPMG data using a non-linear least squares method and linear inverse theory. Magn Reson Med. 1993; 29(6):767–775. [PubMed: 8350719]

Stikov N, Boudreau M, Levesque IR, Tardif CL, Barral JK, Pike GB. On the accuracy of T1 mapping: Searching for common ground. Magn Reson Med. 2014; 73(2):514–522. [PubMed: 24578189]

Stüber C, Morawski M, Schäfer A, Labadie C, Wähnert M, Leuze C, Streicher M, Barapatre N, Reimann K, Geyer S, Spemann D, Turner R. Myelin and iron concentration in the human brain: a quantitative study of MRI contrast. Neuroimage. 2014; 93(Pt 1):95–106. [PubMed: 24607447]

Sumpf TJ, Petrovic A, Uecker M, Knoll F, Frahm J. Fast T2 mapping with improved accuracy using undersampled spin-echo MRI and model-based reconstructions with a generating function. IEEE T Med Imaging. 2014; 33(12):2213–2222.

Sumpf TJ, Uecker M, Boretius S, Frahm J. Model-based nonlinear inverse reconstruction for T2 mapping using highly undersampled spin-echo MRI. J Magn Reson Imaging. 2011; 34(2):420–428. [PubMed: 21780234]

Swift TJ, Fritz OG. A proton spin-echo study of the state of water in frog nerves. Biophys J. 1969; 9(1):54–59. [PubMed: 5782895]

Teixeira RPAG, Malik SJ, Hajnal JV. Joint system relaxometry (JSR) and Crámer-Rao lower bound optimization of sequence parameters: A framework for enhanced precision of DESPOT T1 and T2 estimation. Magn Reson Med. 2018; 79(1):234–245. [PubMed: 28303617]

Travis AR, Does MD. Selective excitation of myelin water using inversion-recovery-based preparations. Magn Reson Med. 2005; 54(3):743–747. [PubMed: 16088884]

van Gelderen P, de Zwart JA, Lee J, Sati P, Reich DS, Duyn JH. Nonexponential T2* decay in white matter. Magn Reson Med. 2012; 67(1):110–117. [PubMed: 21630352]

Vasilescu V, Katona E, Simplăceanu V, Demco D. Water compartments in the myelinated nerve. III. Pulsed NMR results. Experientia. 1978; 34(11):1443–1444. [PubMed: 309823]

Vavasour IM, Huijskens SC, Li DK, Traboulsee AL, Mädler B, Kolind SH, Rauscher A, Moore GW, MacKay AL, Laule C. Global loss of myelin water over 5 years in multiple sclerosis normal-appearing white matter. Mult Scler J. 2017; 84(10):1–12.

Vavasour IM, Laule C, Li DKB, Oger J, Moore GRW, Traboulsee A, MacKay AL. Longitudinal changes in myelin water fraction in two MS patients with active disease. J Neurol Sci. 2009; 276(1–2):49–53. [PubMed: 18822435]

Veraart J, Novikov DS, Fieremans E. TE dependent Diffusion Imaging (TEdDI) distinguishes between compartmental T2 relaxation times. Neuroimage. 2017. URL

Vidarsson L, Conolly SM, Lim KO, Gold GE, Pauly JM. Echo time optimization for linear combination myelin imaging. Magn Reson Med. 2005; 53(2):398–407. [PubMed: 15678534]

Wachowicz K, Snyder RE. Assignment of the T2 components of amphibian peripheral nerve to their microanatomical compartments. Magn Reson Med. 2002; 47(2):239–245. [PubMed: 11810666]

Webb S, Munro C, Midha R, Stanisz G. Is multicomponent T-2 a good measure of myelin content in peripheral nerve? Magn Reson Med. 2003; 49(4):638–645. [PubMed: 12652534]

West KL, Kelm ND, Carson RP, Gochberg DF, Ess KC. Myelin Volume Fraction Imaging with MRI. Neuroimage. 2016. URL

Whittall K, MacKay A, Graeb D, Nugent R, Li D, Paty D. In vivo measurement of T-2 distributions and water contents in normal human brain. Magn Reson Med. 1997; 37(1):34–43. [PubMed: 8978630]

Whittall KP. Recovering compartment sizes from NMR relaxation data. J Magn Reson. 1991; 94(3): 486–492.

Whittall KP, Bronskill MJ, Henkelman RM. Investigation of analysis techniques for complicated NMR relaxation data. J Magn Reson. 1991; 95(2):221–234.

Whittall KP, MacKay AL. Quantitative Interpretation of NMR Relaxation Data. J Magn Reson. 1989; 84:134–152.

Yablonskiy DA. Quantitation of intrinsic magnetic susceptibility-related effects in a tissue matrix. Phantom study. Magn Reson Med. 1998; 39(3):417–428. [PubMed: 9498598]

Zhang J, Kolind SH, Laule C, Mackay AL. Comparison of myelin water fraction from multiecho T2 decay curve and steady-state methods. Magn Reson Med. 2015a; 73(1):223–232. [PubMed: 24515972]

Zhang J, Kolind SH, Laule C, Mackay AL. How does magnetization transfer influence mcDESPOT results? Magn Reson Med. 2015b; 74(5):1327–1335. [PubMed: 25399771]

Zimmerman JR, Brittin WE. Nuclear Magnetic Resonance Studies in Multiple Phase Systems: Lifetime of a Water Molecule in an Adsorbing Phase on Silica Gel. J Phys Chem. 1957; 61(10): 1328–1333.

Highlights

- MRI relaxometry is sensitive to brain tissue microstructure
- Each of T_1, T_2, and T_2^* relaxometry can be used
- Tissue models, acquisition methods, and analysis methods are important

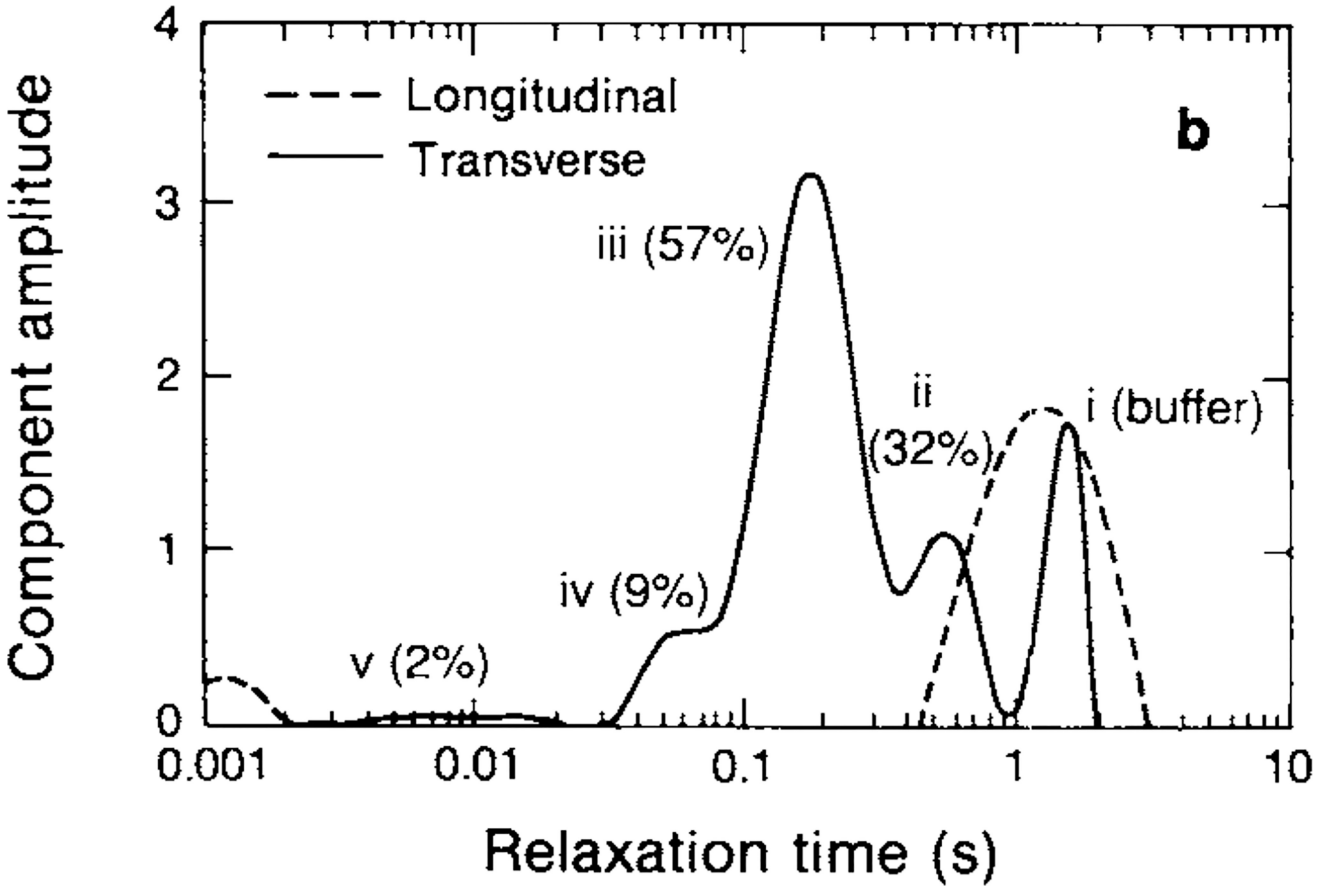

Figure 1.

Representative T_1 and T_2 spectra from crayfish nerve cord. The T_1 spectrum is essentially mono-exponential, presumably reflecting a fast exchange environment, while the T_2 spectrum identifies at least three significant components, thought to be derived from different micro-anatomical compartments. (Menon et al., 1992)

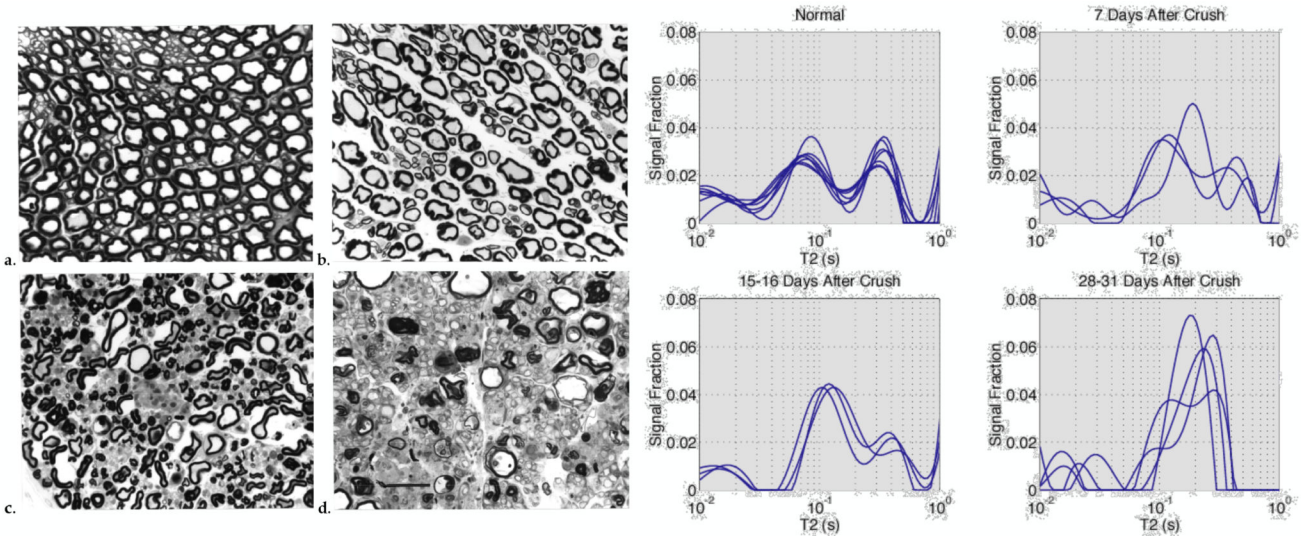

Figure 2.

On the left, representative light microscopic images of frog sciatic nerve at different stages of Wallerian degeneration, and on the right corresponding T_2 spectra from corresponding nerves. As the myelin is removed during the degeneration process, the three-component T_2 spectra collapse toward a mono-exponential function. Adapted, with permission from (Does and Snyder, 1996)

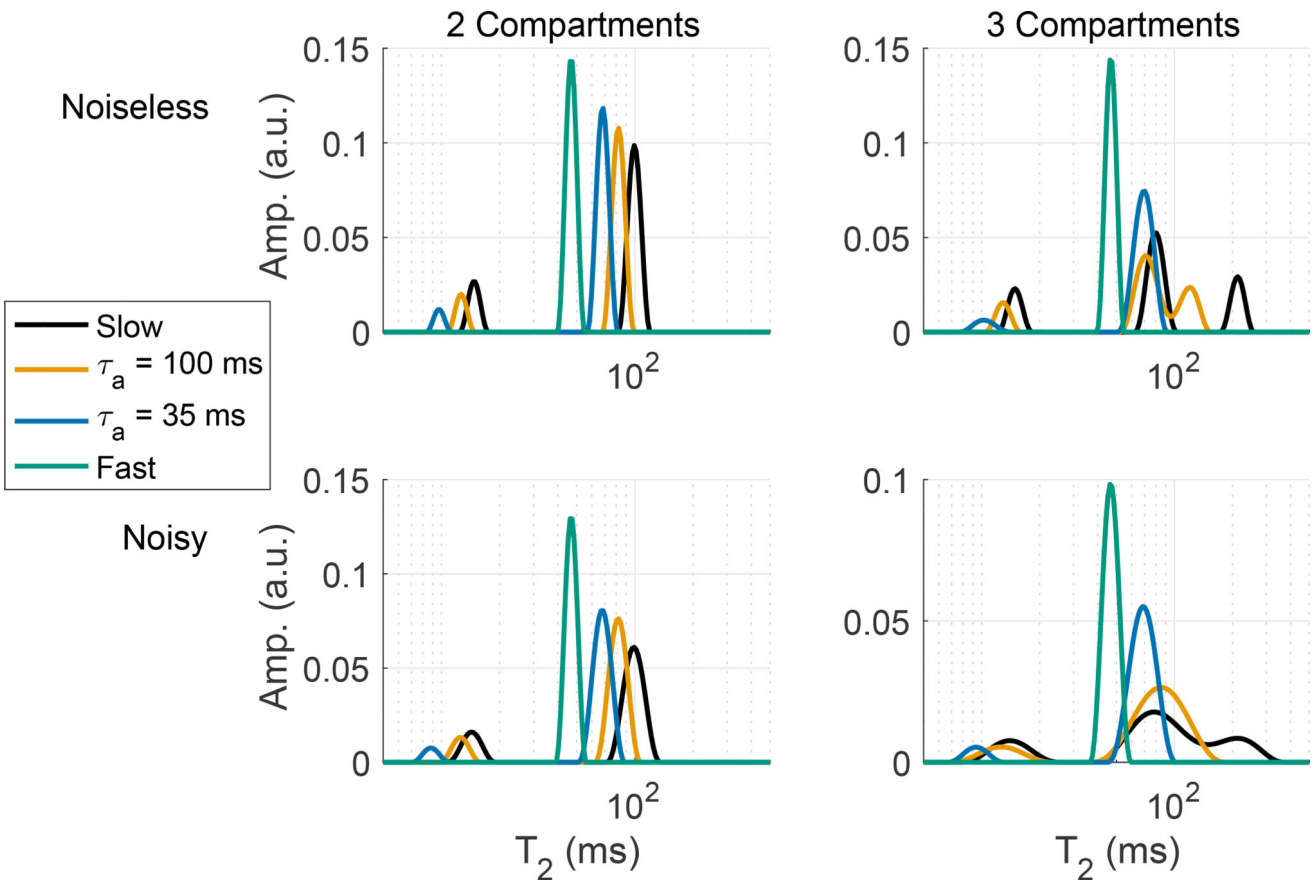

Figure 3.

Example simulated 2- and 3-compartment T_2 spectra, showing how the spectra change with increasing inter-compartmental exchange (decreasing myelin water lifetime, τ_a) and a finite amount of signal noise.

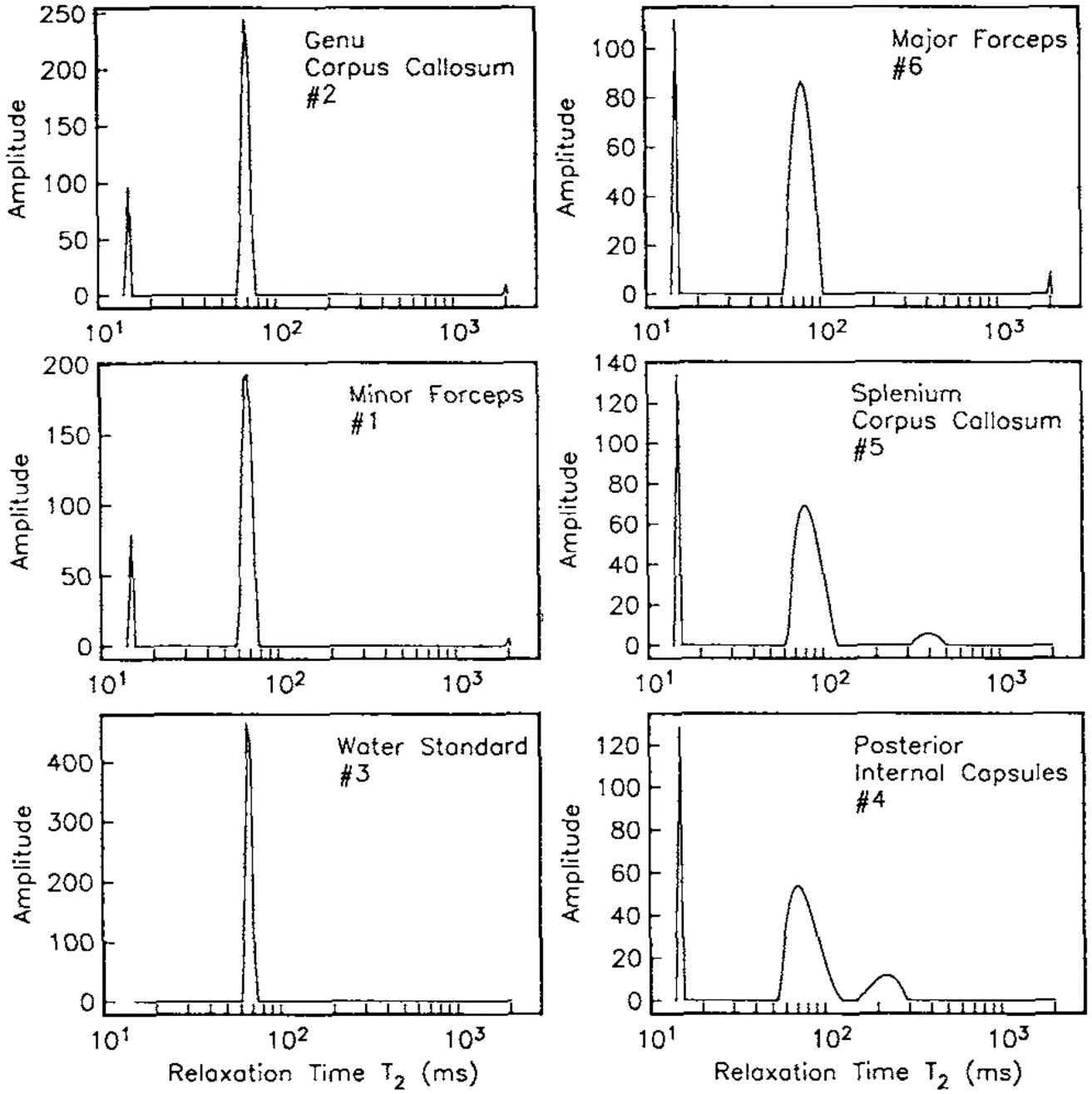

Figure 4.

Representative T_2-spectra from human white matter, in vivo. The spectra show significant variation in the MWF and the long-lived component T_2 values across regions. With permission from (Whittall et al., 1997)